Copyright Warning & Restrictions

The copyright law of the United States (Title 17, United States Code) governs the making of photocopies or other reproductions of copyrighted material.

Under certain conditions specified in the law, libraries and archives are authorized to furnish a photocopy or other reproduction. One of these specified conditions is that the photocopy or reproduction is not to be "used for any purpose other than private study, scholarship, or research." If a, user makes a request for, or later uses, a photocopy or reproduction for purposes in excess of "fair use" that user may be liable for copyright infringement,

This institution reserves the right to refuse to accept a copying order if, in its judgment, fulfillment of the order would involve violation of copyright law.

Please Note: The author retains the copyright while the New Jersey Institute of Technology reserves the right to distribute this thesis or dissertation

Printing note: If you do not wish to print this page, then select "Pages from: first page # to: last page #" on the print dialog screen

ABSTRACT

RECONSTITUTING THE CYANOBACTERIAL CIRCADIAN CLOCK *IN VITRO*

by
Pyong Hwa Kim

Cyanobacteria are photosynthetic organisms that are known to be responsible for oxygenating Earth's early atmosphere. Having evolved to ensure optimal survival in the periodic light/dark cycle on this planet, their genetic codes are packed with various tools, including a sophisticated biological timekeeping system. Among the cyanobacteria is *Synechococcus elongatus* PCC 7942, the simplest clock-harboring organism with a powerful genetic tool that enabled the identification of its intricate timekeeping mechanism. The three central oscillator proteins—KaiA, KaiB, and KaiC—drive the 24 h cyclic gene expression rhythm of cyanobacteria, and the "ticking" of the oscillator can be reconstituted inside a test tube just by mixing the three recombinant proteins with ATP and Mg^{2+}.

Along with its biochemical resilience, the post-translational rhythm of the oscillation can be reset through sensing oxidized quinone, a metabolite that becomes abundant at the onset of darkness. In addition, the output components pick up the information from the central oscillator, tuning the physiological and behavioral patterns and enabling the organism to better cope with the cyclic environmental conditions. In this research, how the cyanobacterial circadian clock functions as a molecular chronometer that readies the host for predictable changes in its surroundings is highlighted and discussed.

Since the bottleneck of performing any *in vitro* experiments is the laborious task of purifying proteins with enough purity, the most efficient method to extract KaiC is introduced, so that other impurities cannot hinder the highly sensitive post-translational activities. Next, CikA, an input component that synchronizes the oscillator to the environmental cues by using a metabolite called “quinone” as a proxy for darkness, is introduced. Finally, KaiC’s C-terminal linear chain undergoes conformational changes that determine the rising or falling phase of the clock. By creating site mutations that constitutively maintain the loop’s exposed conformation, a potentially additional role of another oscillator component, KaiB, is elucidated. Thus, by using the *in vitro* techniques that are compatible with this bacterial clock, the functional details that lie behind the biochemical workings of the circadian clock are disclosed.

RECONSTITUTING THE CYANOBACTERIAL CIRCADIAN CLOCK *IN VITRO*

by
Pyong Hwa Kim

A Dissertation
Submitted to the Faculty of
New Jersey Institute of Technology
in Partial Fulfillment of the Requirements for the Degree of
Doctor of Philosophy in Chemistry

Department of Chemistry and Environmental Science

May 2021

APPROVAL PAGE

RECONSTITUTING THE CYANOBACTERIAL CIRCADIAN CLOCK *IN VITRO*

Pyong Hwa Kim

Dr. Yong-Ick Kim, Dissertation Advisor Assistant Professor of Chemistry, NJIT	Date
Dr. Edgardo T. Farinas, Committee Member Associate Professor of Chemistry, NJIT	Date
Dr. Tamara M. Gund, Committee Member Professor of Chemistry, NJIT	Date
Dr. Yuanwei Zhang, Committee Member Assistant Professor of Chemistry, NJIT	Date
Dr. Casey O. Diekman, Committee Member Associate Professor of Mathematical Sciences, NJIT	Date

BIOGRAPHICAL SKETCH

Author: Pyong Hwa Kim

Degree: Doctor of Philosophy

Date: May 2021

Undergraduate and Graduate Education:

- Doctor of Philosophy in Chemistry,
  New Jersey Institute of Technology, Newark, NJ, 2021

- Bachelor of Science in Biochemical and Biophysical Sciences,
  University of Houston, Houston, TX, 2015

Major: Chemistry

Presentations and Publications:

Pyonghwa Kim, Neha Thati, Hye-In Jang, Yong-Ick Kim, "Shift in Conformational Equilibrium Underlies the Oscillatory Phosphoryl Transfer Reaction in the Circadian Clock" (Submitted)

Pyonghwa Kim and Yong-Ick Kim, "An *In Vitro* Approach to Elucidating Clock-modulating Metabolites," Circadian Rhythms in Bacteria and Microbiomes," Berlin, Germany: Springer, In press

Pyonghwa Kim, Manpreet Kaur, Hye-In Jang, and Yong-Ick Kim, "The Circadian Clock-A Molecular Tool for Survival in Cyanobacteria," Life, 10(12), 365 (2020)

Pyonghwa Kim, Brianna Porr, Tetsuya Mori, Yong-Sung Kim, Carl H. Johnson, Casey O. Diekman, and Yong-Ick Kim, "CikA, an Input Pathway Component, Senses the Oxidized Quinone Signal to Generate Phase Delays in the Cyanobacterial Circadian Clock," Journal of Biological Rhythms, 35(3), 227–234 (2020)

Pyonghwa Kim, Adriana Kaszuba, Hye-In Jang, and Yong-Ick Kim, "Purification of GST-Fused Cyanobacterial Central Oscillator Protein KaiC," Applied Biochemistry and Microbiology, 56(4), 395–399 (2020)

Manpreet Kaur, Amy Ng, Pyonghwa Kim, Casey O. Diekman, Yong-Ick Kim, "CikA Modulates the Effect of KaiA on the Period of the Circadian Oscillation in KaiC Phosphorylation," Journal of Biological Rhythms, 34(2), 218-223 (2019)

Young M. Jeong, Cristiano L. Dias, Casey O. Diekman, Helene Brochon, Pyonghwa Kim, Manpreet Kaur, Yong-Sung Kim, Hye-In Jang, and Yong-Ick Kim, "Magnesium Regulates the Circadian Oscillator in Cyanobacteria," Journal of Biological Rhythms, 34(4), 380-390 (2019)

To Jinhee,
for continuing this journey with me.

ACKNOWLEDGMENT

May I start with Dr. Yong-Ick Kim, my dissertation advisor and academic mentor, who has not only inundated me with in-depth knowledge, but also paved the way to my next step in this journey.

I thank my committee members, Dr. Edgardo Farians, Dr. Tamara Gund, Dr. Yuanwei Zhang, and Dr. Casey Diekman for attentively providing me with critical comments and feedbacks that I sincerely needed for honing my academic skills.

Also, I would like to thank the Department of Chemistry and Environmental Science for funding me as a teaching assistant throughout my stay at NJIT.

This would have been impossible without my colleague, Sarah Young Kim, who has guided me in technical and personal difficulties.

Finally, I would like to acknowledge my wife, Jinhee, who chose to stay with me throughout my study, managed to give birth to our son, Joel, and now became a big part of me.

TABLE OF CONTENTS

TABLE OF CONTENTS
(Continued)

Chapter **Page**

TABLE OF CONTENTS
(Continued)

TABLE OF CONTENTS
(Continued)

Chapter **Page**

LIST OF TABLES

Table **Page**

LIST OF FIGURES

LIST OF FIGURES
(Continued)

Figure **Page**

LIST OF SYMBOLS AND ACHRONYMS

Δ*gene*	A mutant cell line that has the particular *gene* deleted
Q_{10}	A standard measurement of temperature-compensating property in a chemical reaction; $Q_{10} \approx 1.0$ signifies the presence of this property.
Q_0	2,3-Dimethoxy-5-methyl-p-benzoquinone (a quinone analogue)
DBMIB	Dibromothymoquinone (a quinone analogue)
ATP	Adenosine triphosphate
ADP	Adenosine diphosphate
Mg^{2+}	Magnesium ion
≈	Approximately
Å	Angstrom (10^{-10} meters)
H-bond	Hydrogen bond

LIST OF DEFINITIONS

Circadian Time (CT)	The standard unit of time. This is an slightly adjusted time to fit in a 24-h scale, since not all circadian rhythms have an exact 24-h periodicity in various conditions.
Zeitgeber Time (ZT)	A unit of time based on the period of a zeitgeber, such as the 12:12 light:dark cycle. This is an empirical and raw time that often does not have 24-h periodicity.
Entrainment	The process of synchronizing the circadian rhythm to the environmental time in response to a cue by shifting the phase of the oscillation.
Temperature-compensation	A property of reaction rate being relatively irresponsive to temperature change
Free-running	One of the properties of the circadian clock that does not require environmental input to oscillate autonomously
Circadian rhythm	An about-a-day biological rhythm in organisms
Dark pulse	A period of darkness that is applied as to light-detecting cells an environmental cue, often to generate a phase shift
Phase	Angle of the oscillation
Period	The peak-to-peak or trough-to-trough distance in an oscillation
Phase Response Curve (PRC)	Phase responses plotted against the time of day when the dark pulse was administered. Positive and negative values on the graph designate a phase advance and delay respectively

CHAPTER 1

INTRODUCTION

1.1 Objective

Reanimating the cyanobacterial circadian clock in an isolated test tube condition has revealed functional properties that are otherwise difficult to observe *in vivo*, a biochemically noisy environment. The photosynthetic prokaryote's relatively simple oscillator proteins' remarkable resilience in the artificial condition, their temporal association and dissociation, and the post-translational modifications that "free-runs" *in vitro* need further elucidation regarding the additional details that remain in the biological clock mechanism. Adding CikA, quinone, Mg^{2+}, and ATP/ADP into the standard KaiABC *in vitro* mixture may be a major step forward in reconstituting the entire cyanobacterial circadian clock *in vitro*.

In this research, we first streamline the process of purifying the most important oscillator component, KaiC, by eliminating a few steps and lengthening one of the chromatographic washing steps. Next, based on what we recently discovered regarding the competition between KaiA and CikA and their common binding site on KaiB, we add oxidized quinone to the *in vitro* mixture in a temporal manner and introduce a possible mechanism of phase shifting of the cyanobacterial circadian oscillation in response to dark cues. Finally, KaiC has a linear chain that undergoes conformational changes that are key to determining the mode of post-translational modification. By creating the mutations that constitutively maintain phosphorylation activity, we elucidate KaiB's additional role in inducing the initiation of dephosphorylation phase

through exerting an allosteric effect on KaiC.

1.2 Background information

By genetically fusing clock-controlled promoters to the genes for coding bioluminescent proteins, the cyanobacterial circadian clock with its temporally controlled transcriptional/translational activities can be visualized as rhythmic luminescence (Kondo et al., 1993). This powerful genetic tool has provided tremendous insight regarding the visualization of periodic gene expression rhythm (Diamond et al., 2017; Dong et al., 2010; Takai et al., 2006). However, the reporter signal reflects not only rhythmic gene expression, but also the abundance of metabolically active cofactors needed for the bioluminescence reaction (Teng, Mukherji, Moffitt, de Buyl, & O'Shea, 2013). In order to directly monitor the activity of clock proteins and their interaction with metabolites at a molecular level, there must be a way to study the reaction in an isolated condition free from the cellular cacophony.

The circadian clock of the cyanobacterium, *Synechococcus elongatus* PCC 7942 (hereafter *S. elongatus*), composed of a core oscillator of three proteins: KaiA, KaiB, and KaiC. Perhaps two of the milestone discoveries made by Takao Kondo's laboratory that still resonate to this day are that the clock runs through a post-translational mechanism and that this rhythm can be regenerated inside a test tube with only three Kai proteins: adenosine triphosphate (ATP), and magnesium ion (Mg^{2+}), hereafter referred to as the *in vitro* oscillator mixture (Nakajima et al., 2005; Tomita, Nakajima, Kondo, & Iwasaki, 2005). This established that the cyanobacterial circadian clock is a physical and tangible entity that enables its interactions and effects to be directly tested. The sense of

independence from the more prevalent timekeeping mechanisms that fully rely on the transcriptional/translational feedback loop is unlike any other organisms discovered so far.

Among the three Kai proteins, KaiC is perhaps the most interesting one, since it is an enzyme with two biochemically opposing activities that sequentially dominate in a circadian pattern (Kitayama, Nishiwaki, Terauchi, & Kondo, 2008). As a result, KaiC is hyperphosphorylated at dusk and hypophosphorylated at dawn (Iwasaki, Nishiwaki, Kitayama, Nakajima, & Kondo, 2002; Tomita et al., 2005). This is due to KaiC's remarkably slow reaction rate and timely alternation of enzyme activities as autokinase (phosphorylating itself) and autophosphatase (dephosphorylating itself) (Nishiwaki, Iwasaki, Ishiura, & Kondo, 2000; Xu, Mori, & Johnson, 2003). There are two sites of phosphorylation in *S. elongatus* KaiC, and this first occurs at threonine-432 (T432) and serine-431 (S431); dephosphorylation proceeds in a step-wise manner as well, the phosphorylated T432 getting dephosphorylated first and then S431 (Nishiwaki et al., 2007; Rust, Markson, Lane, Fisher, & O'Shea, 2007) (Figure 1.1).

KaiA induces the phosphorylation of KaiC (Iwasaki et al., 2002; Williams, Vakonakis, Golden, & LiWang, 2002) by binding and stabilizing the exposed A-loop conformation of KaiC (Y. I. Kim, Dong, Carruthers, Golden, & LiWang, 2008). KaiC is a hexameric protein composed of two domains, CI and CII (Pattanayek et al., 2004). When the KaiC phosphorylation level peaks (ST-KaiC), its CII domain becomes rigid and is stacked on the CI domain (Chang, Tseng, Kuo, & LiWang, 2012), revealing the KaiB binding site. After KaiC-KaiB complexation takes place, KaiB commences the dephosphorylation phase by sequestering KaiA from the A-loop, slowing down and

reversing the autokinase activity of KaiC (Kitayama, Iwasaki, Nishiwaki, & Kondo, 2003).

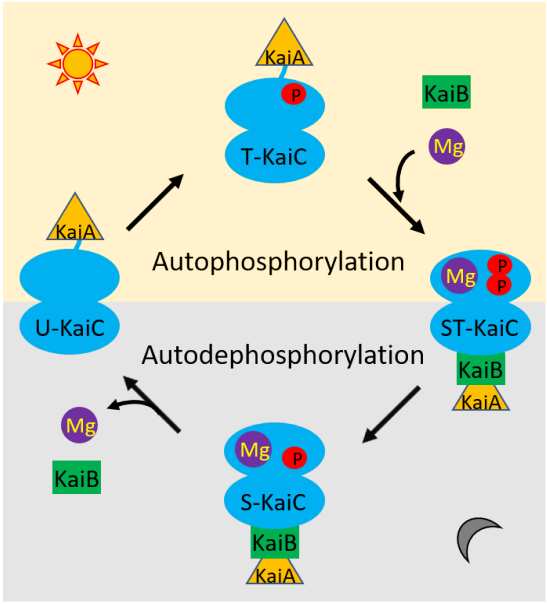

Figure 1.1 The circadian rhythm of the autophosphorylation and autodephosphorylation of KaiC. Day: yellow background, Night: gray background, U-KaiC: unphosphorylated, T-KaiC: phosphorylation on T432, S-KaiC: phosphorylation on S431, ST-KaiC: phosphorylation on both.
Source: P. Kim & Y-I Kim 2021, In press.

S. elongatus KaiC expressed in and purified from *Escherichia coli*—depending on the presence of and incubation time with KaiA and KaiB—is in different phosphorylation states, and each population of the KaiC phosphoforms can be separated and visualized through sodium dodecyl sulfate polyacrylamide gel electrophoresis (SDS-PAGE), where phosphorylated KaiC migrates more slowly (P. Kim, Kaszuba, Jang, & Kim, 2020; Y. I. Kim, Boyd, Espinosa, & Golden, 2015). Through densitometry, the temporally varying ratios between unphosphorylated and phosphorylated KaiC bands can be numerically compared, signifying the phosphorylation state change that can be easily tracked.

Exposing cyanobacteria to a constant light condition helped us to isolate the central oscillator components that sustain the free-running rhythm without environmental cues. However, a single cycle of 12-h light/12-h dark can synchronize any out-of-tune cyanobacteria to oscillate in harmony *in vivo*. The periodic light/dark cycle experienced by cyanobacteria can cause oscillatory abundances in various metabolites. By binding these metabolites only at a certain time of day, the central oscillator components—namely KaiA, CikA, and KaiC—can reset the rhythm of KaiC phosphorylation. The *in vitro* mixture has advanced to the point that the cyanobacterial clock's phase-resetting ability can be tested by directly adding metabolites to the mixture to mimic day and night.

CHAPTER 2

PURIFICATION OF GST-FUSED CYANOBACTERIAL CENTRAL OSCILLATOR PROTEIN KaiC

2.1 Problem Statement

The cyanobacterial circadian clock is the most well-understood and simplest biological time-keeping system. Its oscillator consists of three proteins: KaiA, KaiB, and KaiC. When combined together in a test tube, the Kai proteins produce a free-running 24-h cycle of rhythmic auto-phosphorylation and auto-dephosphorylation. To generate a robust circadian rhythm of the *in vitro* reaction mixture, KaiC, the core oscillator protein, must be purified with an untraditional approach, since even the smallest amount of impurity can hinder its post-translational activities. Until recently, series of fast protein liquid chromatography (FPLC) columns (glutathione S-transferase (GST), anion exchange (Q), and desalting columns) have been used to purify the oscillator proteins, often requiring laborious elution processes. Although the common methodology has already been established, whether the purified KaiC can produce robust oscillations remains to be verified. Here we emphasize the significance of eliminating the Q step and lengthening the duration of washing step for the GST column for generating a rhythmic KaiC phosphorylation *in vitro*. These findings demonstrate the potential for shortening the amount of time and effort it takes to purify proteins without compromising its quality.

The rate-limiting step of *in vitro* study is perhaps purifying proteins with high enough purity which is often found to be a laborious process. Especially in the case of monitoring the temporal changes in clock proteins, it is of utmost importance to prevent

unwanted contamination. This is because ATPases that are naturally present in *Escherichia coli* can not only attenuate the robustness of oscillations through the hydrolysis of ATP in the mixture, but also disturb the KaiC's hexameric complexation, a process which also requires ATP. Moreover, a small amount of natural impurities, such as proteases, can degrade the Kai proteins, which results in the disruption of oscillation (Y. I. Kim et al., 2015).

Several methods have already been established, although neither providing enough details for purifying KaiC nor validating their protocols. Initially, Nakajima with coworkers introduced the ways to reconstitute the biological clock in a test tube and monitor its post-translational activity as time progresses (Nakajima et al., 2005). Here we produce a robust *in vitro* circadian oscillation using the KaiC protein purified in accordance with the methodology that Kim with coauthors previously published (Y. I. Kim et al., 2015), confirming its reliability and usefulness for further related studies. Some minor improvements - the omission of Q column elution step and elongation of GST washing step, are introduced in this paper as a further refinement of currently available methods.

2.2 Materials and Methods

2.2.1 Expression of KaiC

GST-tagged KaiC domain was amplified through PCR and then ligated into a T7-inducible pET-41a(+) vector (Novagen, Germany) between *NcoI* and *HindIII* restriction sites (Mittal, Misra, Owais, & Goyal, 2005). After the plasmid was verified through DNA sequencing, it was transformed in *E. coli* (BL21DES, Novagen, Germany) and

bacteria were grown in 1 L of Luria Bertani (LB) medium (Thermo-Fisher Scientific, USA) containing kanamycin (32.5 μg/mL) at 37˚C. When OD_{600} of the culture reached 7.0, the temperature was lowered to 25˚C. Then 100 mM IPTG was added to induce overexpression of KaiC, and the culture was incubated for additional 16 h. Cells were harvested by centrifugation at 5500 × g for 10 min. Cell pellets were resuspended in 60 mL of loading buffer (50 mM Tris-HCl buffer containing 150 mM NaCl, 5 mM $MgCl_2$, 1 mM EDTA, 5 mM ATP, and 1 mM DTT; pH 7.3) and lysed by passing through a chilled French press (Glen Mills, USA) at a constant rate of 16,000 psi. The lysates were centrifuged at 20,000 × g for 2 h and filtered through a 0.45 μm filter (Thermo-Fisher Scientific, USA).

2.2.2 Purification of KaiC

The separation of GST-tagged KaiC from crude cell lysate was achieved by first equilibrating a prepacked 5-mL GST column (GSTrap HP, GE Healthcare, USA) with 25 mL of the loading buffer and injecting 60 mL of the cell lysate into it. To assess the efficacy of using our modified method to purify KaiC, two samples of KaiC were purified. The first sample (*KaiC_arrhythmic*) utilized the typical washing step (removing the non-specifically bound impurities on the column by injecting the loading buffer after the sample injection) of 30 mL at 1 mL/min (2-6 volumes) as outlined in the original KaiC purification protocol (Nishiwaki et al., 2004). The second sample (*KaiC_rhythmic*) was purified using the proposed lengthened washing period using 100 mL of the loading buffer at 1 mL/min (20 volumes) (Y. I. Kim et al., 2015). An ÄKTA start (GE Healthcare, USA), FPLC system was used for the purification of KaiC. This FPLC system consisted of a pump, pressure sensor, UV monitor, and conductivity

monitor, which could be operated at a pressure of up to 5 bar. The elution buffer contained 50 mM Tris-HCl buffer (pH 7.3) supplemented with 150 mM NaCl, 5 mM $MgCl_2$, 1 mM EDTA, 1 mM ATP, 1 mM DTT and 6 mM glutathione, the competitive ligand to GST-tagged KaiC. The GST-column was washed after use by flushing the column with 4 resin volumes of ddH_2O, 4 resin volumes of 70% ethanol, 4 resin volumes of ddH_2O, 2 resin volumes of guanidine-HCl, and again resin volumes of ddH_2O. Columns were stored at 4˚C when not in use. The overall lifetime of the column has not been determined.

After the sample elution, PreScission™ protease (GE Healthcare, USA) was used to cleave the GST-tags from KaiC. Additionally, HiPrap 26/10 desalting columns from GE Healthcare (USA) were used for desalting steps. The final KaiC protein isolate was obtained through the use of another GST column, where digested GST-tags were separated from KaiC in solution. Bradford reagent (Alfa Aesar, USA) was used with small samples of the final KaiC isolate to measure the protein concentration based on a predetermined standard curve. The protein samples were run individually through a 10% SDS-polyacrylamide gel to verify that each contains KaiC.

2.2.3 Reconstitution and visualization of KaiC phosphorylation rhythm

After performing *in vitro* reactions and aliquoting samples at evenly spaced time intervals, the phosphorylation states of the samples were visualized through SDS-PAGE and subsequent staining using InstantBlue™ Coomassie stain (Expedeon, Germany). The *in vitro* reaction mixture was prepared by mixing 1.2 μM KaiA, 3.5 μM KaiB, 3.5 μM KaiC, 1 mM ATP, 5 mM $MgCl_2$, 150 mM NaCl, 0.5 mM EDTA, and 50 mM Tris-HCl buffer (pH 8.0) (Tomita et al., 2005). After aliquoting from each reaction during

evenly spaced 2-h time points over the span of 72 h, the samples were denatured at 90 ^{o}C for 3 min, run on a 6.5% SDS-polyacrylamide gel, and analyzed by constructing a densitometric graph of phosphorylation states. KaiA and KaiB were purified as previously reported (Y. I. Kim et al., 2015).

2.3 Results and Discussion

2.3.1 Eliminating the Q column step

To compare and evaluate the protein functionalities achieved by varying each washing period length, both samples omitted the use of a Q column were treated in the same manner in two separate but identical *in vitro* reaction mixture. As per the traditional method, a Q column is used primarily to remove ATPases (Nishiwaki et al., 2004). For example, Hsp70 molecular chaperones, DnaK, an impurity reported to abolish the circadian oscillation of KaiC phosphorylation by consuming ATP *in vitro,* is commonly expressed in *E. coli* along with many GST fusion proteins. It has been shown to be removed through the use of Q column (Rial & Ceccarelli, 2002), but in efforts to reduce the amount of time and resources needed to purify KaiC, we eliminated this step in which Q column is used on the basis that a lengthened washing period through a GST column with 5 mM ATP at 30°C may enable sufficient separation to be achieved in one step, as outlined in Figure 2.1. The desalting step, which would have been needed to change the buffer following the usage of the Q column, was subsequently removed as well. Thus, our modified purification protocol requires only the usage of two types of columns - GST column and desalting column.

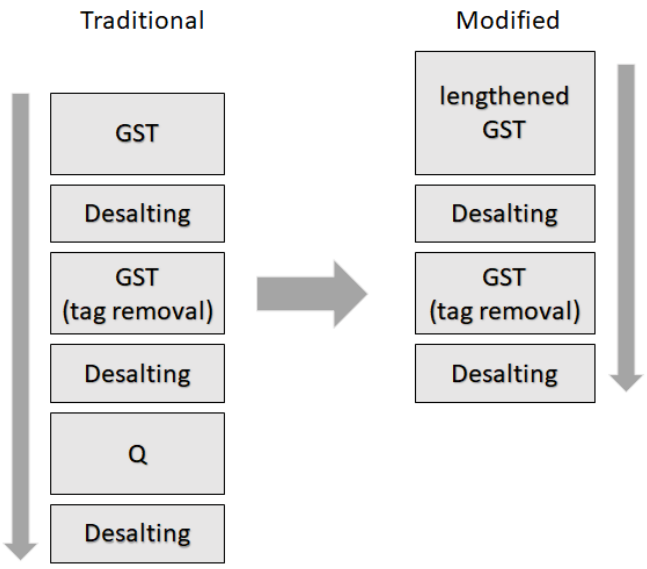

Figure 2.1 Comparison of the traditional (left) and modified (right) KaiC purification methods.
Source: P. Kim, Kaszuba, et al., 2020

Additionally, this method can be cheaper and less time-consuming, since the Q column and buffer solutions would no longer be needed. The Q column, which involves utilizing a salt gradient in the separation of molecules on the basis of their charge, may be omitted in light of this study's results due to sufficient removal of impurities from the GST column during a prolonged washing period. The use of fewer columns during purification procedure provides many benefits, including convenience. In addition, by using a lesser number of columns, this method potentially minimizes any sample loss that may occur when switching columns. Our typical yield for purified KaiC was 0.3 g/L.

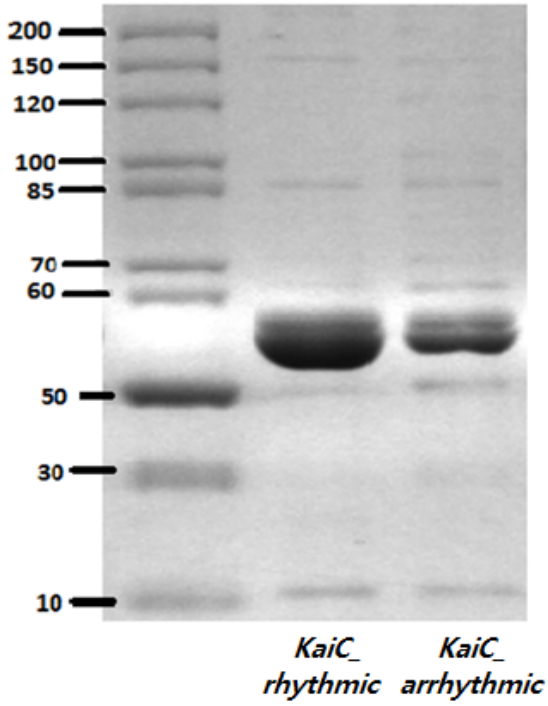

Figure 2.2. Comparison of purities between *KaiC_rhythmic* and *KaiC_arrhythmic* KaiC samples on 10% SDS-polyacrylamide gel. The increased degree of separation achieved with 10% gels, allows for visualization of trace proteins within *KaiC_rhythmic* and *KaiC_arrhythmic* samples. A protein ladder was run alongside two samples.
Source: P. Kim, Kaszuba, et al., 2020

2.3.2 Prolonged washing periods of KaiC purification

To maximize the purity of the final protein sample, we increased the washing period during which an impure protein sample is passed through the first GST column. Loading *KaiC_rhythmic* and *KaiC_arrhythmic* on the 10% gel confirms the presence of KaiC achieved by the two washing period lengths (Figure 2.2). The increased degree of separation achieved with 10% gels, allowed for visualization of trace proteins within the samples. *KaiC_rhythmic* was eluted for 200 min, and *KaiC_arrhythmic* for 120 min total. The arrhythmic oscillation of *KaiC_arrhythmic* suggests that the shorter washing period was less effective in isolating the target species, probably due to a larger amount of contaminants recovered during fractionation (Figure 2.3). The impact of prolonged

washing periods in affinity chromatography procedures was explored for the purification of KaiC. The two purification protocols sought to demonstrate whether significantly lengthening the washing period after which a target substance is bound to an affinity matrix could prove to be an effective alternative to using multiple types of columns, including Q column, in series when purifying a protein. To represent the oscillations of the circadian rhythm, a densitometric graph was constructed using the densitometric ratio of phosphorylated KaiC to total KaiC and plotting the value as a function of the incubation time is shown in Figure 2.3. The occluded oscillations generated by *KaiC_arrhythmic* suggest poor separation of KaiC during the shorter washing period, which can likely be attributed to the insufficient removal of impurities from the column. It is apparent that the *KaiC_rhythmic* reaction exhibits more consistent periods of oscillation than the *KaiC_arrhythmic* reaction, which fails to re-phosphorylate after 12 h. Comparing these results, the longer washing period appears to be better suited for purifying KaiC, whereas *KaiC_arrhythmic* would require the use of a Q column for further separation.

This traditional method for KaiC purification is a time-consuming process that may require a technician's supervision over a span of 4-5 h. Lengthening the washing period through which the loading buffer is passed through the GST column to wash off everything but GST-tagged KaiC proved to be successful in purifying KaiC for reconstituting the cyanobacterial circadian rhythm *in vitro*, despite not utilizing a Q column as dictated by the traditional method of purification (Chen, Liu, Yang, Zhang, & Li, 2018; Kitayama et al., 2003; Mukaiyama, Ouyang, Furuike, & Akiyama, 2019; Nishiwaki et al., 2007; Snijder et al., 2014). Further research on KaiC's structural and

functional analysis would improve the methods to purify the protein.

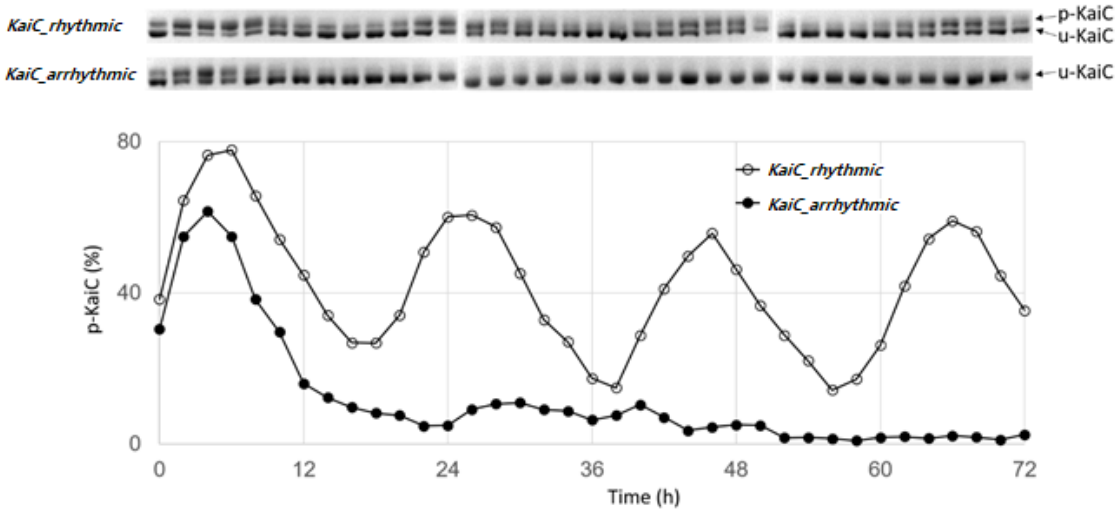

Figure 2.3 *In vitro* oscillations of *KaiC_rhythmic* and *KaiC_arrhythmic* KaiC samples. *KaiC_rhythmic* and *KaiC_arrhythmic* samples were incubated with KaiA and KaiB in the presence of ATP and $MgCl_2$ in two separate reactions. Aliquots of each reaction mixture were collected every 2 h over a span of 72 h to visualize the phosphorylation and dephosphorylation cycle of the two KaiC samples. Aliquots were denatured and ran in a 6.5% SDS-polyacrylamide gel to visualize auto-phosphorylation and auto-dephosphorylation of KaiC. A densitometric analysis of data was constructed using the ratios of phosphorylated KaiC to total KaiC to visualize circadian rhythm oscillations.
Source: P. Kim, Kaszuba, et al., 2020

In this research, the original chromatographic method to purify KaiC was further improved. This study ultimately credits prolonging the washing period during affinity chromatography procedures as a reliable approach to simplifying existing purification protocols for KaiC. Key parameters relevant to this method included significantly extending the washing period of the stationary phase in which GST-tagged KaiC is bound to the GST column and omitting the Q step. This resulted in a purified KaiC sample that successfully reconstituted the circadian rhythm.

CHAPTER 3

CikA, AN INPUT PATHWAY COMPONENT, SENSES THE OXIDIZED QUINONE SIGNAL TO GENERATE PHASE DELAYS IN THE CYANOBACTERIAL CIRCADIAN CLOCK

3.1 Background Information

3.1.1 Modulating the circadian clock with adenosine diphosphate (ADP)

Ideally, the circadian clock must be robust enough to withstand cellular noise and simultaneously sensitive to environmental cues for rapidly responding to stimuli. The alignment of the phase of free-running circadian rhythm to the appropriate environmental time of day is referred to as entrainment. Since *S. elongatus* relies on light as a source of energy and cannot survive without it, virtually all cellular activities except housekeeping genes are shut down in the absence of light. Therefore, a dark pulse of 4-5 hours is applied to the synchronized culture grown in a constant light environment in order to monitor the obligate phototroph's ability to reset its cellular rhythm (Kiyohara, Katayama, & Kondo, 2005). Depending on the timing of the dark-pulse application, the phase of KaiC's post-translational oscillation can shift forward (phase advance) or backward (phase delay). This effect is summarized in a phase response curve (PRC), which displays phase responses plotted against the time of day when the dark pulse was administered (Johnson, 1999). Positive and negative values on the graph designate a phase advance and delay, respectively (Figure. 3.1). In cyanobacteria, a dark pulse generates an extreme phase shift if applied during the rising phase of the clock, forcing the oscillation to shift its phase; conversely, it does not cause extreme phase shifts in gene expression rhythm only if applied during the falling phase.

Additionally, if a dark pulse is applied at Circadian Time [CT] 8, the phase advances the most; if applied between CT 18 and CT 24, the phase delays (Kiyohara et al., 2005).

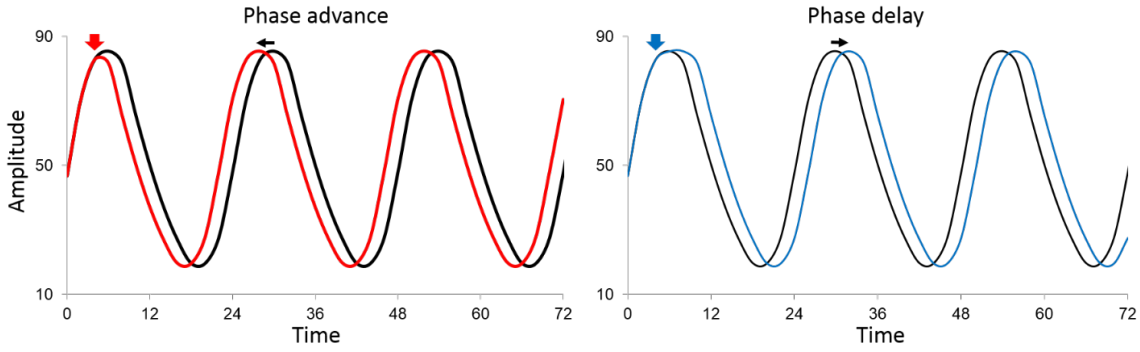

Figure 3.1 Representative illustration of phase shifts (phase advance and phase delay). The black lines are the oscillations without dark pulse. The red and blue lines are the oscillations influenced by a dark pulse. The red and blue arrows indicate the time points of the input signal. The black arrows show the directions of the phase shifts.
Source: P. Kim & Y-I Kim 2021, In press.

Then, how is the information about light or darkness conveyed to the cell to entrain the central oscillator in a phase-dependent manner? Rust et al. showed that varying ATP/ADP ratio successfully mimicked the application of dark pulse by generating both a phase advance and delay of the KaiC phosphorylation rhythm (Rust, Golden, & O'Shea, 2011). The mechanism behind this remarkable discovery is partly that the cyclic KaiC phosphorylation can be modulated by the availability of ATP as a substrate both *in vivo* and *in vitro*. When the cell is rich with ATP during the day, the phosphorylation of KaiC dominates, while its dephosphorylation can take over when ADP becomes relatively more available at night and competes with ATP for binding KaiC. The variations in endogenous and *in vitro* ATP/ADP ratio directly affects KaiC and modulates its phosphorylation rhythm, bypassing the input pathway. However, variations in the ATP/ADP ratio brought about by the onset of darkness become

apparent only after 2 to 3 hours *in vivo* (Rust et al., 2011). Moreover in another study, although the endogenous level of glycogen oscillated in both 12-h light/12-h dark and constant light, the changes in endogenous energy charge ratio brought about by darkness seem relatively trivial (Puszynska & O'Shea, 2017). While KaiC's sensing of ATP/ADP ratio is biologically significant when it comes to long-term synchronization, it is insufficient to fully explain *S. elongatus*' more acute response to a dark pulse in resetting the circadian clock (Kiyohara et al., 2005).

3.1.2 Resetting the clock through sensing the redox state of quinone

Perhaps it was this particular missing gap between input and the central oscillator that urged the search for light-sensing input components in cyanobacteria. Plants sense light through a protein called phytochrome, which binds a chromophore called bilin, and relays the information to its circadian clock (Montgomery & Lagarias, 2002). A sequencing revealed some similarity with the protein CikA, originally discovered in a screen for *S. elongatus* mutants that do not phase shift appropriately in response to a dark pulse in cyanobacteria, even though one of CikA's domains was missing a canonical motif important in signal transduction (Schmitz, Katayama, Williams, Kondo, & Golden, 2000). This enigmatic receiver-like C-terminal domain was named pseudo-receiver (PsR) domain because it was missing the conserved phosphate-accepting aspartyl residue. Several attempts were made to find a partner component that binds to PsR, although an *in vivo* chromophore-binding assay for CikA gave out a negative result (Mutsuda, Michel, Zhang, Montgomery, & Golden, 2003); when the effect of photosynthesis on the circadian clock was being examined, a quinone analog was identified as a possible PsR-interacting metabolite (Ivleva, Bramlett, Lindahl, & Golden,

2005; Ivleva, Gao, LiWang, & Golden, 2006).

Instead of spatially separating biochemically incompatible yet vital metabolic reactions, cyanobacteria—unlike plants—perform oxygenic photosynthesis and respiration in the same compartment (Mullineaux, 2014). Notice that these are two opposite processes; photosynthesis converts CO_2 and water into sugars using sunlight, and respiration converts sugars into CO_2 and water fueling the much needed reducing power at night. Therefore, it would make sense that the *de novo* synthesis of photosystems, ATP synthase, carbon fixation-related proteins peaks at dawn (Diamond *et al*., 2017; Ito *et al*., 2009; Vijayan, Zuzow, & O'Shea, 2009). Although the absence of light could signify the end of a solar energy source, it could mean a life and death situation without the ability to sense and prepare for the imminent darkness. When the sun sets, an alternative source of reducing power comes from breaking down glycogen that has been stored inside the cell. Thus, it was suggested that the inability to prepare the necessary proteins for metabolizing glycogen at night underlie the lethal effect of a clock mutation that requires constant light condition (Markson, Piechura, Puszynska, & O'Shea, 2013; Puszynska & O'Shea, 2017). This means that the cyanobacteria with a dysfunctional output component that failed to stock up on energy and run the backup generator in time did not last the night. Intuitivively, the quickest and most efficient way to transduce this vital information about incoming darkness to the cell would be from photosystem directly to the endogenous clock.

As potential ancestors of plants, cyanobacteria use quinone to shuttle electrons from both photosynthetic and respiratory electron transports. Surprisingly, the cellular level of reduced quinone drops abruptly as compared to a more gradual decrease in the

ATP/ADP ratio. This redox-balancing of the plastoquinone (PQ) pool in *S. elongatus* is visualized in a fast repetition rate fluorescence measured during a simulated diurnal cycle (Y. I. Kim, Vinyard, Ananyev, Dismukes, & Golden, 2012). In response to the onset of darkness, it produced a very sharp peak and a gradual return to its moderately reduced state, signifying abrupt oxidation of the PQ pool and an eventual influx of backup reducing power, probably from glycogen breakdown. This established that there is a transient yet definite abundance of oxidized quinone in *S. elongatus* at the onset of darkness.

As a result of the initiation and termination of photosynthesis, the PQ pool is reduced and oxidized respectively. How does this change in overall redox state communicated to the cell? The quinone analog DBMIB (2,5-dibromo-3-methyl-6-isopropyl-p-benzoquinone)—which affects the redox state of the cellular PQ pool in photosynthetic organisms—is often used as an electron transport inhibitor that tightly binds b6f complex and prevents reoxidation of the reduced PQ pool (Escoubas, Lomas, LaRoche, & Falkowski, 1995). Moreover, The addition of oxidized DBMIB decreases the stability of CikA and KaiA, confirming their role in redox-sensing (Ivleva *et al*., 2005). The measurement of chemical shift perturbations induced by the binding of DBMIB to CikA's PsR domain structurally confirmed that CikA binds the quinone analog (Gao, Zhang, Ivleva, Golden, & LiWang, 2007; Mutsuda *et al*., 2003), and KaiA too has a structurally similar N-terminal PsR domain that can bind quinone (Pattanayek, Sidiqi, & Egli, 2012; Vakonakis *et al*., 2004).

Since adding oxidized DBMIB can mimic the onset of darkness, sodium dithionite—a reducing agent—can be used to mimic the dark-to-light transition, so that oxidized DBMIB can be reduced back to its inactive form. Indeed, an *in vitro* experiment showed that KaiA stimulation of KaiC phosphorylation was blocked only when oxidized DBMIB was added; conversely, KaiA had no problem stimulating KaiC phosphorylation when DBMIB was reduced with sodium dithionite before the addition (Wood *et al.*, 2010). Moreover, neither KaiA nor CikA underwent degradation when reduced DBMIB was added *in vivo*, thus proving their selective sensitivity for oxidized quinone.

More surprising was the phase-dependent effect of adding oxidized quinone. After considering DBMIB's relatively low redox potential (thus a tendency to resist reduction), another quinone analog Q_0 (2,3-Dimethoxy-5-methyl-p-benzoquinone) was used from this point and was added to the *in vitro* mixture to mimic the onset of darkness (Y. I. Kim *et al.*, 2012). First, adding Q_0 to cyanobacterial cultures caused the oxidation of PQ pool and shifted the phase of the bioluminescence rhythm in a phase-dependent manner, in agreement with the *in vivo* PRC of 4-h dark pulse application. To biochemically mimic the application of 4-h dark pulse *in vitro*, Q_0 was applied to signify the onset of darkness. After 4 hours, sodium dithionite was added to reduce the quinone back to its inactive form, marking the end of darkness. The initial *in vitro* mixture without CikA could generate a phase advance in response to a 4-h oxidized Q_0 application.

On the other hand, a phase delay was not generated in the expected range, and thus the *in vitro* reconstitution of quinone entrainment remained somewhat inadequate. It was reasoned that quinone's inactivation of KaiA during the autokinase-dominant phase of KaiC leads to premature dephosphorylation and hence a phase advance—its effect peaking at CT 8—although only speculations remained regarding CikA's supposed role in delaying the phase for a while. Could this phase-dependent effect of quinone sensing be recapitulated in the expanded *in vitro* mixture that contains CikA? This issue was clarified by molecular snapshots that provided a structural basis for KaiA's and CikA's binding interactions with the binary KaiB-KaiC complex (Tseng *et al.*, 2017). Considering that KaiB only binds phosphorylated KaiC, the effect of CikA's competition with KaiA for binding KaiB would take place in the dephosphorylating phase. Thus, KaiA and CikA seem to compete with each other and adding CikA into the KaiABC mixture may affect the KaiC phosphorylation as an input component.

When the concentration of CikA was increased in the *in vitro* mixture, the overall level of KaiC phosphorylation was raised and the period shortened as if KaiA were in excess. Our interpretation is that free KaiA, released by competing with CikA for its common spot on KaiB, became more available for readily binding back to the A-loop and stimulating the KaiC phosphorylation. More importantly, when the KaiA concentration was reduced, a similar level of increase in CikA concentration offset and buffered the expected period lengthening, retaining the same period length that is normally affected by changes in KaiA concentration. This indicates that CikA compensates for low KaiA concentration, shielding its period lengthening effect (M. Kaur, A. Ng, P. Kim, C. Diekman, & Y. I. Kim, 2019). An input component receives

and transduces the temporal information to the central oscillator by aligning its self-running rhythm to that of the environment. The input functionality of CikA was clearly demonstrated after it was shown that CikA is an important component that generates a phase delay in response to a dark pulse (P. Kim, Porr, *et al.*, 2020). But isn't the competition between KaiA and CikA a contradictory argument against the shortened periodicity of *ΔcikA*? Amidst the presence of other biological players including LdpA that are known to interact with CikA, it is difficult to explain the short period of *ΔcikA* by this point (Mackey *et al.*, 2008). This means that an absence of CikA would in theory lead to KaiA inactivation and period lengthening in the deletion mutant. Another possibility is that CikA could affect gene expression rhythm as an output component (Gutu & O'Shea, 2013). As we slowly uncover the detailed mechanism behind additional functionalities of CikA and CikA-interacting proteins, we must never presume CikA's competing manner is its sole biological characteristic. However, there is no doubt that the competition with KaiA is one of CikA's multifaceted features, as increasing the PsR domain of CikA shortened the circadian rhythm both *in vivo* and *in vitro* (Chang *et al.*, 2015; Zhang, Dong, & Golden, 2006).

3.2 Materials and Methods

3.2.1 Phosphorylation assay of the circadian clock *in vitro*

Cloning, purifications, and phosphorylation assays were performed as described previously without modification (M. Kaur *et al.*, 2019; Y. I. Kim *et al.*, 2015). CikA was cloned into pET41a(+) vector, expressed in E.coli (BL21DE3), and purified with a GST affinity column using the same method as for KaiC (Y. I. Kim et al., 2015). The *in*

vitro oscillation mixtures were prepared with the Kai proteins and CikA in the circadian oscillation buffer (150 mM NaCl, 20 mM Tris-HCl, 5 mM $MgCl_2$, 0.5 mM EDTA, 1 mM ATP, pH 8.0). Each 20 μL oscillation mixture was collected in every 2-h intervals for 2 or 3 days. The collected samples were denatured immediately by adding SDS-gel loading dye (100 mM Tris·HCl, pH 6.8, 4% SDS, 0.2% bromophenol blue, 20% glycerol, 400 mM β-mercaptoethanol) and kept in -20°C. 6.5% SDS-PAGE was used to separate the phosphorylated and unphosphorylated KaiC. ImageJ (NIH) was used for the densitometry (Schindelin *et al.*, 2012). Periods and phases were estimated using Biodare2 (https://biodare2.ed.ac.uk/) implementation of the fast Fourier transform-nonlinear least squares (FFT-NLLS) procedure with linear detrending (Zielinski, Moore, Troup, Halliday, & Millar, 2014).

3.2.2 Statistical analysis of the periods

Dunnett's test was used to compare the period of oscillations under different treatments (CikA concentrations) to a control (absence of CikA). This test was performed using the DunnettTest function in the R package 'DescTools' with R version 3.5.1 (Signorell *et al.*, 2019). Tukey's Honest Significance Difference method was used to perform pairwise comparisons of the period of oscillations at different temperatures. This test was implemented using the TukeyHSD function in the R package 'stats' (R Core Team, 2018).

3.2.3 Quinone entrainment assay

Quinone entrainment assays were performed as described previously (Y. I. Kim *et al.*, 2012) with the following modification: For the oscillation mixture, we used 10 mM

ATP concentration to remove the effect of the ADP/ATP ratio (Rust *et al.*, 2011). The oscillation mixtures were incubated overnight at 30°C without KaiA and CikA to make KaiC fully dephosphorylate. The time 0 sample was collected immediately after adding KaiA and CikA. Q_0 (2,3-Dimethoxy-5-methyl-p-benzoquinone) was added to the oscillation mixtures to mimic the beginning of the dark pulse. After 4 hours, dithionite (200 μM final concentration) was added to reduce Q_0 for mimicking the termination of the dark pulse. The final concentration of quinone was 9.6 μM for every entrainment experiment. The later 2 days' (from 28 h to 72 h) data were used for phase estimation.

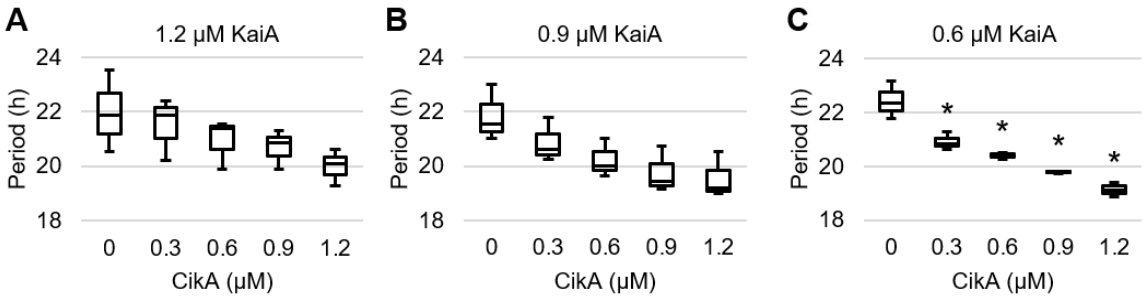

Figure 3.2 Statistical analysis of the circadian period with various CikA and KaiA concentrations. The concentration of KaiA is labeled on top of the graph and 3.4 μM KaiB and 3.4 μM KaiC were used to generate the oscillation. (A) The period data are taken from the published article (M. Kaur, A. Ng, P. Kim, C. Diekman, & Y.-I. Kim, 2019). (B) No statistically significant change was observed among the periods. (C) An asterisk indicates that the period is significantly different from that of 0 μM CikA. $P < 0.01$. n=3.
Source: P. Kim, Porr, et al., 2020

3.3 Results

3.3.1 Adding CikA compensates a decrease in KaiA concentration in maintaining the period of the circadian oscillation reaction mixture

Because various amounts of KaiA and CikA are known to affect the period and amplitude of the circadian oscillation of KaiC phosphorylation (Kageyama *et al.*, 2006;

M. Kaur *et al.*, 2019), we tried to find the minimum CikA concentration that gives a statistically meaningful effect on the period. Various amounts of CikA (from 0.3 μM to 1.2 μM) were added into the circadian oscillation mixture with various amounts of KaiA (from 0.3 μM to 1.2 μM) and each phosphorylation state of KaiC was monitored for 2 days. The period of each oscillation mixture was estimated and statistically analyzed to find a concentration that leads to the maximum effect on the period (Figure 3.2, Table A.1). With 1.2 μM and 0.9 μM KaiA, we did not find any statistically meaningful change in the period when increasing CikA concentration (Figure 3.2A, 3.2B, A.1). We also did not consider the 0.3 μM KaiA concentration because the amplitudes of the oscillations were not robust enough (Figure A.1). The 0.6 μM CikA and 0.6 μM KaiA concentration was selected for further experimentation because it shows a statistically meaningful change and a relatively conserved circadian period (Figure 3.2C, A.1). One of the criteria for being considered a circadian oscillator is a period near 24 hours in a constant environment, and this reaction mixture fulfills that requirement.

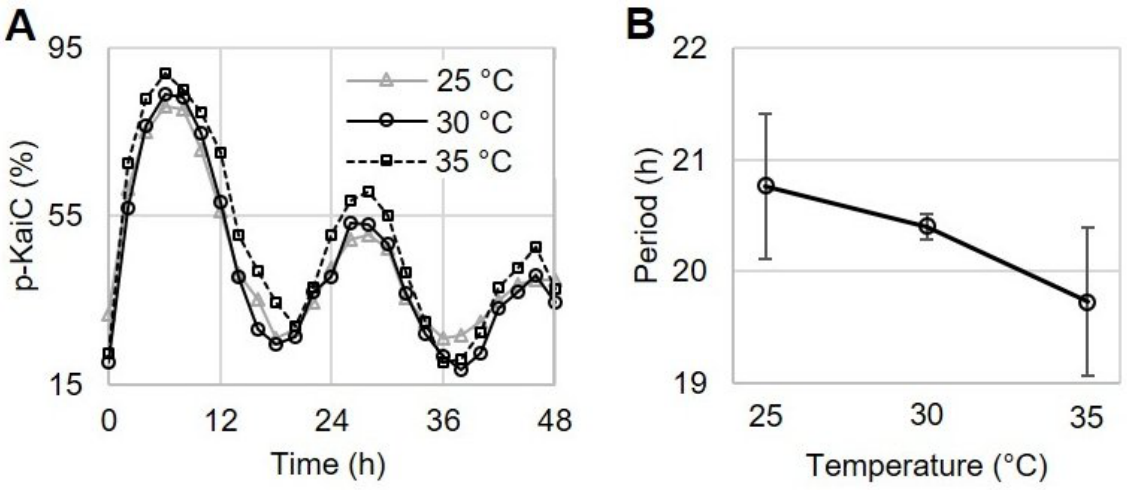

Figure 3.3 Temperature compensation of the circadian clock *in vitro*. (A) The circadian oscillations of KaiC phosphorylation at the different temperatures. (B) The circadian

periods of the circadian clock *in vitro* at different temperatures. Error bars are standard deviation (SD). n=3.
Source: P. Kim, Porr, et al., 2020

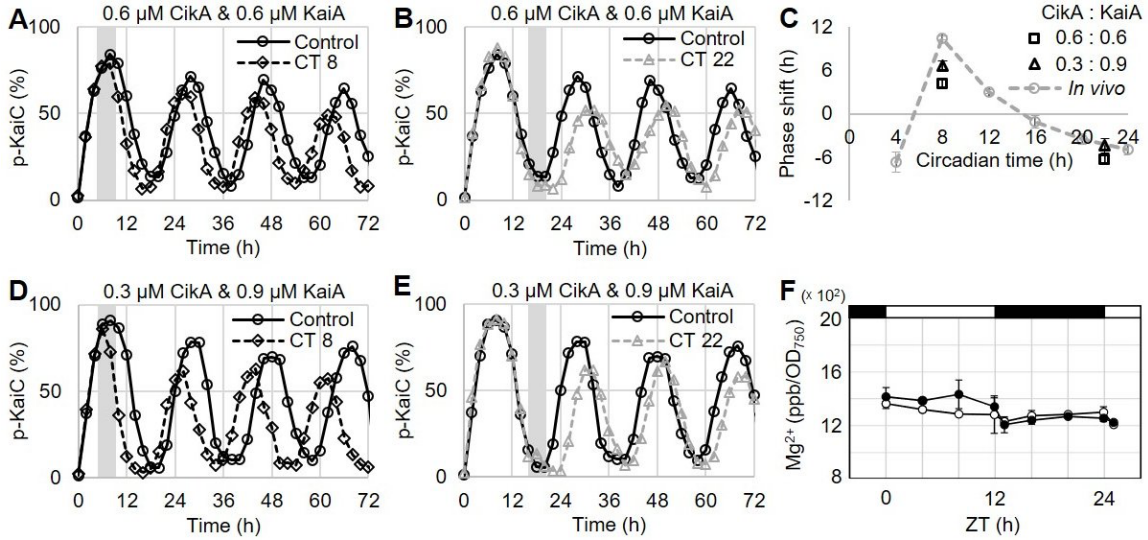

Figure 3.4 Entrainment of the circadian clock *in vitro* and total magnesium concentration *in vivo*. (A) The quinone entrainment of the KaiC phosphorylation at CT 8. The gray bar represents the duration of adding oxidized quinone in the circadian clock mixture *in vitro*. (B) The quinone entrainment of the KaiC phosphorylation at CT 22. (C) The PRC of the cyanobacterial circadian clock *in vitro* and *in vivo*. Error bars are standard errors of the mean (SEM). n=3. (D) The quinone entrainment of the KaiC phosphorylation at CT 8. (E) The quinone entrainment of the KaiC phosphorylation at CT 22. (F) Total magnesium concentration in cyanobacteria: wild-type (○) and *ΔkaiABC* (●). error bars show the standard deviation (SD). n=3.
Source: P. Kim, Porr, et al., 2020

3.3.2 The temperature compensation of the period was conserved in the new cyanobacterial circadian clock mixture with an input component, CikA

To test the temperature compensation of this reaction mixture (0.6 μM CikA, 0.6 μM KaiA, 3.4 μM KaiB, and 3.4 μM KaiC), the oscillation periods were measured at 25°C and 35°C. Robust circadian oscillations were observed at all temperatures and periods were conserved in the circadian range (Figure 3.3A, A.2). The periods increased when the temperature decreased (Figure 3.3B, Table A.2), however the change in period was not statistically significant (Table A.3). This is the same trend that was previously

reported without CikA in the reaction mixture (Nakajima *et al.*, 2005). The temperature compensation was examined by calculating the Q_{10} value of the circadian clock reaction mixtures using the periods at 25°C and 35°C. The Q_{10} value was 0.95 for the new circadian clock mixture meaning that adding CikA and decreasing KaiA did not change the property of the temperature compensation. Therefore, our reaction mixture with CikA fulfills another requirement of a circadian clock.

3.3.3 The new circadian clock mixture showed both phase advance and phase delay on the PRC in response to the oxidized quinone signal

The last requirement is that a circadian clock must be entrainable. To test this with quinone, we selected the 0.6 μM CikA and 0.6 μM KaiA concentrations that conserve the temperature compensation of the circadian period. The phosphorylation of KaiC can be suppressed by adding 9.6 μM quinone (Figure A.3). Quinone entrainment experiments were performed at circadian time (CT) 8 (Figure 3.4A, A.3) and CT 22 (Figure 3.4B, A.3) to observe the phase advance (at CT 8) and delay (at CT 22) by adding oxidized quinone in the circadian clock mixture for 4 hours. When oxidized quinone was applied at CT 8, a 4-h phase advance was observed (Figure 3.4C). This phase advance was smaller than that in the previous report which used the circadian oscillator without an input component (Y. I. Kim *et al.*, 2012). The comparatively less KaiA present in our new reaction mixture may generate less of a phase advance in response to quinone because it is known that KaiA deactivation through quinone binding leads to a phase advance (Y. I. Kim *et al.*, 2012). On the other hand, applying oxidized quinone at CT 22 generated a 6-h phase delay (Figure 3.4C), which was not observed in the experiments without an input component (Y. I. Kim et al., 2012). This

6-h phase delay was 2 hours longer than the PRC generated *in vivo* (Kiyohara *et al.*, 2005). We thought that this difference might to be due to excess CikA present in our reaction mixture. In accordance with our observations, we hypothesized that KaiA and CikA are involved in phase advances and delays, respectively. If we increase KaiA and decrease CikA in our circadian clock mixture, we may observe a PRC that more closely matches the *in vivo* PRC.

3.3.4 KaiA and CikA are involved in the phase advance and delay, respectively

To test our hypothesis, we performed the quinone entrainment experiments with a different ratio of KaiA and CikA. KaiA concentration was increased to 0.9 μM, while CikA concentration was decreased to 0.3 μM because we assume that the amount of the phase shift is positively correlated with the amount of each protein. The summed amount of KaiA and CikA was maintained at 1.2 μM to conserve the circadian period (M. Kaur *et al.*, 2019). In this mixture, a 7-h phase advance and a 4-h phase delay were observed at CT 8 and at CT 22, respectively (Figure 3.4C, 3.4D, 3.4E, A.4). These results are close to the PRC from the *in vivo* study and indicate that the amount of phase advance and phase delay are positively correlated with the concentrations of the KaiA and CikA, respectively. We also performed the control entrainment experiments with the same reaction mixture above but without CikA. The same as the previous report, a 7-h phase advance and no phase delay were observed at CT 8 and at CT 22, respectively (Figure A.5).

3.3.5 Oxidized quinone binding causes a conformational change in the pseudo-receiver domain of CikA, the binding interface of the KaiB binding

To find the effect of quinone on the binding interaction between CikA and KaiB, we analyzed two CikA structures previously published (Gao *et al.*, 2007; Tseng *et al.*, 2017). The pseudo-receiver domain of CikA uses α1 and β2 in order to bind to KaiB (Tseng *et al.*, 2017). A single mutation on α1 of CikA shows the clock phenotype in the same manner as *ΔcikA*, and this indicates that the mutation attenuates the binding affinity between CikA and KaiB (Tseng *et al.*, 2017). Interestingly, when oxidized quinone binds to the pseudo-receiver domain of CikA, conformational changes on α1 and β2 were detected through nuclear magnetic resonance (NMR) spectroscopy (Ivleva *et al.*, 2006). We mapped the disrupted residues on the pseudo-receiver domain of CikA and found that most of the residues are located on α1 and β2 (Figure A.6). Therefore, adding oxidized quinone disrupts the binding interface of CikA and dissociates CikA from KaiB.

3.4 Discussion

Our new data agree with the *in vivo* PRC, based on their structural and binding information of the clock components and quinone. To understand the cyanobacteria's ability to align its circadian clock to environmental cycles, entrainment studies have been performed *in vitro* using only two metabolites so far—ADP and quinone. While the ADP signal works with the oscillator itself through bypassing the input pathway, the quinone signal seemed flawed without the input pathway (Y. I. Kim *et al.*, 2012; Rust *et al.*, 2011). Our *in vitro* results showed that the input pathway is necessary for producing the expected phase delay in the entrainment using quinone signaling.

In the absence of CikA, applying oxidized quinone cannot generate the phase delay (Figure A.5). The inactivation of KaiA at the low level of KaiC phosphorylation may have a minimal effect on the overall KaiC phosphorylation because its phosphorylation level can be recovered after reducing quinone (Figure A.7). However, in the presence of CikA, oxidized quinone dissociates CikA from KaiB and the premature phosphorylation is inhibited (M. Kaur *et al.*, 2019). Also, the inactivation of KaiA keeps KaiC continuously dephosphorylated. After reducing quinone, the system may follow the oscillation phase trajectory of the one in the absence of CikA generating the phase delay (Figure A.7). This idea can be tested by developing an enhanced mathematical model of the system.

Although we still do not understand why *ΔcikA* shows the short-period phenotype *in vivo* (Zhang *et al.*, 2006), CikA is also known to possess an output functionality (Gutu & O'Shea, 2013) that perhaps contributes to the period shortening. This question may be answered if we can reconstitute the entire circadian clock *in vitro* with both the input and output components. Our finding here will serve as a basis for the reconstitution of the entire circadian clock *in vitro*.

CHAPTER 4

SHIFT IN CONFORMATIONAL EQUILIBRIUM UNDERLIES THE OSCILLATORY PHOSPHORYL TRANSFER REACTION OF KAIC

4.1 Background Information

4.1.1 Regulating the KaiC autokinase and autophosphatase activities with Mg^{2+}

Circadian rhythms in endogenous Mg^{2+} have been observed in an algae Ostreococcus tauri and humans, and increasing the exogenous Mg^{2+} concentration leads to lengthening of the circadian period and vice versa (Feeney *et al.*, 2016). Plant chloroplasts display light-dependent fluctuations in cytoplasmic Mg^{2+} concentration, and the Mg^{2+} transporter protein in the thylakoid membrane pumps in and out in response to the darkness and light respectively (Lyu & Lazar, 2017). A similar mechanism could be possible for *S. elongatus* which might have developed a unique timekeeping mechanism for its endogenous Mg^{2+} concentration to oscillate. In a similar manner for the *in vitro* mixture, the removal and addition of Mg^{2+} were performed to simulate light and dark alterations in Mg^{2+} concentrations.

In the C-terminal domain of KaiC, there is a protruding tentacle-like peptide (residue 488-518 in *S. elongatus*) where KaiA binds (Pattanayek *et al.*, 2006; Vakonakis & LiWang, 2004). The upper part of this chain (residue 488-497) is snugly folded inside KaiC by default but, when KaiA is around, wraps around KaiA and stays stretched—hence the name "A-loop" (Y. I. Kim *et al.*, 2008). When KaiA binds KaiC, the A-loop stays unraveled and KaiC autophosphorylates; when KaiA detaches, perhaps as a result of being sequestered by KaiB, the A-loop buries itself into KaiC, and KaiC enters the

dephosphorylation phase. Thus, it was established that the conformational state of A-loop is a determinant factor that modulates KaiC's phosphorylation and dephosphorylation. Interestingly, mutants of KaiC that has its A-loop truncated at residue 487 and 497 (hereafter $KaiC^{\Delta 487}$ and $KaiC^{\Delta 497}$) stay fully phosphorylated and dephosphorylated, respectively, regardless of the presence or absence of KaiA. It was reasoned that $KaiC^{\Delta 487}$'s constitutively high phosphorylation level is attributed to the missing A-loop mimicking its exposed conformation, while $KaiC^{\Delta 497}$'s inability to become phosphorylated even in the presence of KaiA is due to the A-loop being buried inside KaiC and losing access by KaiA. This mutation study further bolstered the notion of A-loop's conformation as a key player in KaiC's rhythmic phosphorylation. The A-loop's regulatory conformational change is thought to affect the phosphorylation sites indirectly through the allosteric effect because the distance from the A-loop to the active site is too far (≈25 Å) to exert a direct effect. After analyzing the crystal structure of KaiC, we noticed that E318, which is known as a catalytic glutamate, is forming a coordination bond with Mg^{2+} and this could hinder its activation of T432 for the phosphoryl-transfer reaction (Egli *et al.*, 2012; Pattanayek *et al.*, 2009).

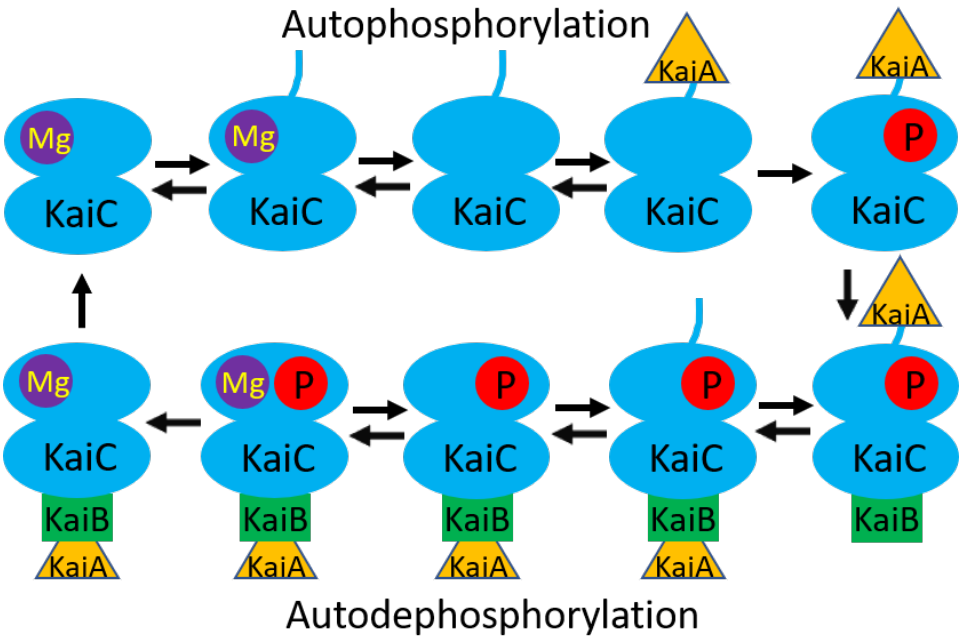

Figure 4.1 The circadian rhythm of KaiC autophosphorylation (red P on KaiC) and autodephosphorylation. When the A-loop (blue tentacle in KaiC) is exposed, the Mg^{2+} dissociates and KaiA stabilizes the A-loop conformation. KaiC is phosphorylated when the Mg^{2+} concentration is low. When KaiC is fully phosphorylated, KaiB binds to KaiC, and KaiA is sequestrated from the A-loop. When the A-loop is buried, Mg^{2+} binds to KaiC and autodephosphorylation starts. KaiB and KaiA dissociate from KaiC when it is fully dephosphorylated to start a new cycle.
Source: P. Kim & Y-I Kim 2021, In press.

In light of this, we varied the concentration of Mg^{2+} in the *in vitro* mixture and observed its hidden role in affecting the central oscillator: an increase in Mg^{2+} caused KaiC dephosphorylation and decreasing it led to phosphorylation (Jeong *et al.*, 2019), in agreement with the previous report (Egli *et al.*, 2012). To determine at which step Mg^{2+} exerts its effect on the KaiC phosphorylation, we used $KaiC^{\Delta 497}$, which lacks the A-loop interaction with KaiA and thus irresponsive to its stimulation of autokinase activity. Decreasing the Mg^{2+} concentration made $KaiC^{\Delta 497}$ become fully phosphorylated even without KaiA. This means that even though the A-loop conformation was locked to the buried state to induce constitutive dephosphorylation, the absence of Mg^{2+} limited its

influence. We reasoned that modulation of the KaiC phosphorylation state by Mg^{2+} is downstream of the A-loop's conformational change (Figure 4.1). Also, E318's mutation into aspartic acid (E318D, a slightly shorter chain) significantly slowed down the KaiC autokinase activity (Jeong et al., 2019). We argue that when the A-loop conformation of wild-type KaiC stays exposed through binding with KaiA, Mg^{2+} could dissociate from the active site of KaiC, allowing E318's rotating motion which in turn activates T432 for phosphorylation.

Take our speculation with a grain of salt, since Mg^{2+} is known to play important roles in other essential metabolic activities unrelated to the clock, including as the central metal of chlorophyll. Along with *ΔcikA*, *ΔkaiB* and $KaiC^{\Delta 487}$, in arrhythmic mutants in which KaiC shows a constitutively high ATPase activity, the cell division gate remains closed and the cell elongates indefinitely (Dong et al., 2010). However, *S. elongatus* grown in a Mg^{2+}-deficient medium reportedly showed an elongated cell phenotype (Utkilen, 1982), a sign suggestive of defective gating of cell division and broken timing circuit (Dong et al., 2010). All other Mg^{2+}-dependent metabolic activities aside, we hypothesize that low cytoplasmic concentration of Mg^{2+} can leave enough freedom for E318's turning motion and place the bound ATP molecule within T432's reach, constitutively phosphorylating KaiC and enhancing its ATPase activity, which in turn closes the cell division gate and leaves the cell elongated in a Mg^{2+}-deficient medium (Dong et al., 2010; Utkilen, 1982).

4.1.2 Keeping time with KaiC alone as an hourglass

What is unique about having a circadian clock as compared to other less intricate time-keeping mechanisms is that it can be distinguished from externally driven oscillations

that only depend on daily environmental cues. This difference between a circadian clock and an hourglass, a time-keeping mechanism lacking an ability to self-run, becomes prominent when the cell is exposed to a constant environment. The conclusion that a circadian clock renders the organism with anticipatory behavior, thus a competitive edge, can be drawn only if the time-keeping mechanism is truly self-running, that is independent of the variations in outside conditions (Ouyang, Andersson, Kondo, Golden, & Johnson, 1998). Less intricate time-keeping systems oscillate merely by reacting to the changes in environmental cues such as light or darkness, while a true circadian clock recalibrates its already free-running rhythm to them (Johnson, Zhao, Xu, & Mori, 2017). For *S. elongatus*, the advantage of having a KaiABC-based post-translational oscillator is that it can self-run without any other biological feedback from the cell.

Not all cyanobacteria are lucky to have such a sophisticated and robust timekeeper. Among the central oscillator components, *kaiC* is thought to be the oldest, while *kaiA* being the youngest (V. Dvornyk, Vinogradova, & Nevo, 2003). ATP and ADP that vary in abundance depending on the time of day directly affect KaiC phosphorylation as a substrate and competitive inhibitor and bypass the input pathway, a seemingly older and more universal metabolite-sensing process. We have explored the effect of quinone as a photochemical metabolite that can be sensed by KaiA and CikA, and this quinone-sensing ability might have been a relatively recent addition to the clock, since it seems to be exclusive to the sophisticated timekeepers, such as that of *S. elongatus* (Volodymyr Dvornyk, 2009).

On the other hand, a change in Mg^{2+} concentration can modulate the rhythm *in vitro*, a process directly affecting KaiC phosphorylation independent of KaiA or KaiB. To sustain the KaiC phosphorylation rhythm only using Mg^{2+} without KaiA or KaiB *in vitro*, Mg^{2+} level is required to oscillate periodically, and this signifies that KaiC by itself cannot free-run without an environmental cue (Jeong et al., 2019). Our computational simulation produced a KaiC-only post-translational oscillation as robust as that of KaiABC-oscillator when the cyclic Mg^{2+} fluctuation was coupled with day-and-night ATP/ADP variation, further pointing at the distant origins of these two clock-tuning sensors. Hence, we argue that KaiC's ability to sense Mg^{2+} may work in KaiC-only hourglass systems as a supposedly primeval cue-dependent process, although the effort to trace this evolutionary trait *in vivo* is still in progress (Figure 4.2).

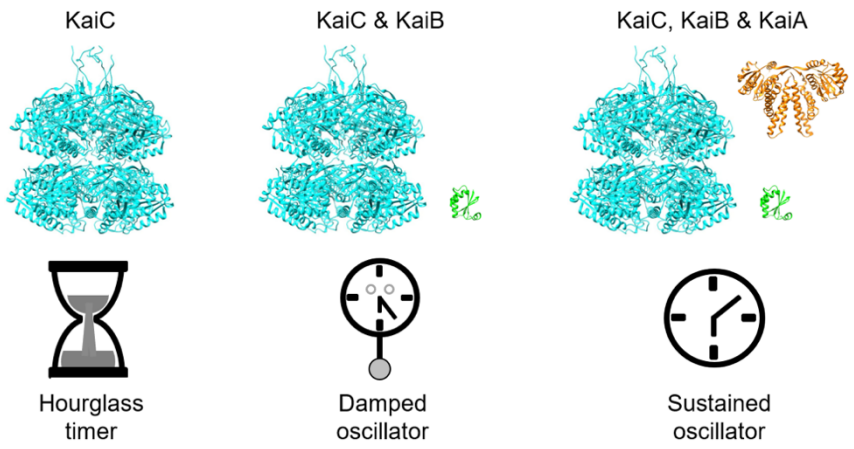

Figure 4.2 A possible evolutionary track of the circadian oscillator in cyanobacteria. KaiC-only system might have evolved into KaiBC system and eventually a self-running KaiABC timekeeper.
Source: P. Kim & Y-I Kim 2021, In press.

The structural and biological level of detail involving the role of Mg^{2+} is rudimentary since there is not enough data in relation to our findings. Perhaps before the ability to control the steady-state level of endogenous Mg^{2+} was established, the periodic

variation in Mg^{2+} concentration in the environment could have served as an environmental cue. The Mg^{2+} concentration in seawater hundreds of millions of years ago is estimated to around half of today's level (Horita, Zimmermann, & Holland, 2002). Although none of us were alive to tell, Mg^{2+} was probably even more scarce billions of years ago, and its periodic fluctuation could have had larger implications in survival than now. Because Mg^{2+} physico-chemically forms relatively weak complexes with organic molecules, its intracellular abundance must be carefully modulated (Waldron, Rutherford, Ford, & Robinson, 2009). Evaporation of water during the day would bring the Mg^{2+} level up at dusk, while condensation at night could bring it down at dawn. Moreover, warm water contains less dissolved oxygen than cool water, and metal concentration in the water may rise with increasing temperature since fewer metals are bound to sediment colloids at low redox potentials (Förstner & Wittmann, 1979). Perhaps as waters became saltier and Mg^{2+} more readily available, Mg^{2+} homeostasis would have been established with priority to contain its fluctuation in the cytoplasm for better survival. Decreasing complexity of sensing various molecules as environmental cues may enable the endogenous rhythm to withstand noise, especially so if its biological implication is great yet its fluctuation no longer relevant, and this seems to be the case at least in *S. elongatus*. More structural and functional studies in other species of clock-harboring bacteria must be done in order to prove or disprove our hypothesis.

Initially, we thought that Mg^{2+} can be a signaling molecule for entrainment if its free-ionic concentration in the cell fluctuates in a temporal manner in response to periodic environmental variations. Unfortunately, in a recent study, *S. elongatus* did not

show significant rhythmic fluctuations in endogenous Mg^{2+} concentration in response to light/dark cycle (P. Kim, Porr, et al., 2020), leaving its relevance and meaning questionable. This negative result is due to *S. elongatus*' high cellular content of Mg^{2+} and fast homeostatic response, hinting at its biological importance. In the future, a method to more selectively detect Mg^{2+} apart from other divalent metal ions would help us to monitor its temporal endogenous fluctuation in *S. elongatus*, if ever. In addition, it would be interesting to observe if there is a change in—if not the total endogenous Mg^{2+} level—the cytoplasmic concentration, since plants show such variation in a light-dependent manner. There are putative candidates for the Mg^{2+} transporter protein in *S. elongatus* PCC 7942, namely *Synpcc7942_1371* and *Synpcc7942_1269* which show sequence homology with *corA* and *mgtE* respectively (Pohland & Schneider, 2019), although at which membrane they are present is still a mystery. It would be intriguing to test the effect of overexpressing or limiting their expression on the cytoplasmic Mg^{2+} fluctuation since KaiC is known to be located in the cytosol (Kitayama et al., 2003). Moreover, it is still possible that endogenous Mg^{2+} fluctuation can be observed in other *kaiC*-possessing cyanobacteria that might have developed a less efficient Mg^{2+} homeostatic response. We are constantly looking for the potential remnants of past pre-homeostatic behavior that can provide us a glimpse of evolutionary history regarding which sequential developmental steps have led to today's cyanobacterial clock and through which mechanistic step the information about light, metabolites, and metal ions is communicated to the central oscillator.

4.1.3 KaiC's inter-A-loop hydrogen bonds stabilize its buried conformation

Amidst growing global concerns over green-house gas emissions and potential energy crisis, a growing number of studies are focusing on the possible ways to harvest electrons (Lea-Smith, Bombelli, Vasudevan, & Howe, 2016; Shah, Garg, & Madamwar, 2001) and chemicals (Ducat, Way, & Silver, 2011; Nozzi, Oliver, & Atsumi, 2013) from cyanobacteria through bioengineering, since for billions of years they have been using sustainable solar energy to capture carbon dioxide and split water, contributing to the oxygenic atmosphere that we breathe today without giving them much of the credit they deserve (Kasting & Siefert, 2002). Among them is *S. elongatus*, of which a significant portion of its physiology is regulated by a circadian clock, so that the expression light-harvesting proteins peaks just before the sunrise and that of proteins needed for breaking down stored glycogen peaks right before the sunset (Diamond et al., 2017; Ito et al., 2009; Vijayan et al., 2009).

Equipped with the biological intricacy that provides a fitness advantage in a rhythmically oscillating environment (Ouyang et al., 1998), cyanobacteria has a central oscillator that is composed of three proteins—KaiA, KaiB, and KaiC—which generate cyclic phosphorylation and dephosphorylation of KaiC with a ≈24-h periodicity (Ishiura et al., 1998). KaiC displays both autokinase and autophosphatase activities regulated by the conformation of its C-terminal peptide called "A-loop"(Vakonakis & LiWang, 2004; Williams et al., 2002). The two conformations (exposed and buried) of the A-loop equilibrate dynamically (Figure B.1), triggering yet another structural variation in the active sites of KaiC (Jeong et al., 2019; Y. I. Kim et al., 2008). We have previously suggested that this latter arrangement modulates the binding affinity of magnesium ion

(Mg^{2+}), which in turn regulates the autokinase and autophosphatase activities in KaiC (Egli et al., 2012; Jeong et al., 2019). When the A-loop is exposed, the Mg^{2+} binding affinity decreases and the autokinase activity is activated (Y. I. Kim et al., 2008). On the other hand, the autophosphatase is activated when the A-loop takes the buried conformation and increases the affinity for binding Mg^{2+} in the active sites (Jeong et al., 2019). KaiA shifts the dynamic equilibrium of the A-loop toward the exposed state by binding to its unraveled form. This conformational locking induces dissociation of Mg^{2+} from the active sites and initiates KaiC autophosphorylation. On the other hand, KaiB induces dephosphorylation by sequestrating KaiA from the A-loop, shifting the dynamic equilibrium toward the buried conformation, supposedly due to a decrease in the abundance of free KaiA (Chang et al., 2015; Y. I. Kim et al., 2008).

Surprisingly, this unusual biological oscillatory system can be reconstituted in a test tube by mixing the three Kai proteins with ATP (P. Kim, Kaszuba, et al., 2020; Y. I. Kim et al., 2015; Nakajima et al., 2005). By examining the simple oscillatory reaction *in vitro*, the role of KaiA has been elucidated comparatively well but that of KaiB is known to be limited to sequestering KaiA so far. To study the function of KaiB on the oscillatory phosphorylation and dephosphorylation of KaiC, studies have been performed with the three-component KaiABC system, although its complexity can hinder attempts to isolate the role of an individual component. In this paper, we applied three alanine mutations individually on the A-loop's hydrogen bonding (H-bonding) residues that are known to stabilize its buried conformation to shift the equilibrium toward the exposed conformation, so that each mutant KaiC displays a constitutively phosphorylated state even without KaiA. Using these KaiC mutants to reconstitute the

two-component KaiBC systems *in vitro* enabled us to investigate the role of KaiB more thoroughly in the circadian oscillator.

4.2 Results

4.2.1 Breaking H-bonds between the A-loops induces the KaiC phosphorylation

The autokinase activity of KaiC is regulated by the conformation of its A-loop (Y. I. Kim et al., 2008). In the hexameric KaiC, the buried conformation of A-loop is stabilized by forming inter- and intra-subunit H-bonds, and breaking these interactions enhances the chance to stay exposed (Egli et al., 2013; Tseng et al., 2014). This dynamic conformational equilibrium affects the Mg^{2+} binding in the active sites, resulting in the regulation of the autophosphorylation or autodephosphorylation of KaiC (Jeong et al., 2019). To observe the H-bonding effect on the KaiC phosphorylation, we analyzed the crystal structure of KaiC (PDBID:1TF7) (Pattanayek et al., 2004) and selected three putative H-bond forming residues (E487, R488, and T495) on the A-loop for mutation studies (Figure B.2). By replacing the original residues to alanine, the H-bonds may be broken in the hexameric KaiC. With three KaiC mutants - KaiC-E487A (thereafter $KaiC^{E487A}$), KaiC-R488A (thereafter $KaiC^{R488A}$), and KaiC-T495A (thereafter $KaiC^{T495A}$), reaction mixtures were reconstituted by following the established *in vitro* protocol to monitor the phosphorylation states (Y. I. Kim et al., 2015). In the absence of KaiA and KaiB, $KaiC^{E487A}$ (Figure 4.3A) and $KaiC^{T495A}$ (Figure 4.3B) started phosphorylation at the beginning of the reaction and kept hyper-phosphorylated (> 95% phosphorylation) for two days. However, $KaiC^{R488A}$ (Figure 4.3C) underwent phosphorylation for the first 2 hours (although the change is not significant) and slowly dephosphorylated for 12 hours until it reached ≈50% phosphorylation level.

In general, to stimulate KaiC phosphorylation *in vitro*, KaiA should be added in the regular reaction mixture(Y. I. Kim et al., 2015; Nakajima et al., 2005) or Mg^{2+} concentration should be lowered in the absence of ethylenediaminetetraacetic acid (EDTA) (Jeong et al., 2019). By breaking the H-bonds on the A-loop of KaiC, the kinase activity can be activated without adding KaiA. From this result, we propose that breaking the H-bonds shifts the dynamic equilibrium of A-loop conformation toward the exposed conformation for $KaiC^{E487A}$ and $KaiC^{T495A}$, which activates the autokinase activity and suppress the autophosphatase activity normally present in wild type KaiC (Figure B.3). Based on the phosphorylation profile, we can predict that E487 and T495 form strong H-bonds while R488 makes comparatively weak H-bonds in A-loop.

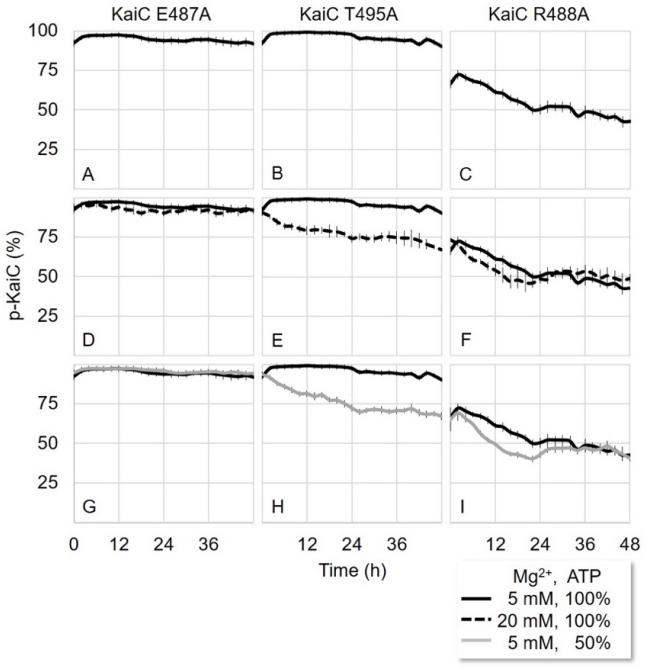

Figure 4.3 Breaking the H-bond network on the A-loop induces the phosphorylation of KaiC mutants. (A-I) All reactions are performed in the same buffer condition (150 mM NaCl, 20 mM Tris-HCl, 5 mM $MgCl_2$, 0.5 mM EDTA, 1 mM ATP, pH = 8.0), if the concentration is not specified. KaiC (3.4 μM) was the only protein in the reaction mixture. Graphs are the average of the two or three replicates. Vertical bars are the standard errors of the mean (SEM) on the time points.
Source: P. Kim et al., Submitted

4.2.2 The KaiC dephosphorylation was enhanced in high Mg^{2+} concentration

KaiC also has autophosphatase activity in addition to autokinase. We previously reported that Mg^{2+} concentration is a crucial factor that regulates autokinase and autophosphatase activity (Jeong et al., 2019). In the low or high concentration of Mg^{2+}, KaiC phosphorylates or dephosphorylates respectively, even without KaiA and KaiB. To observe the Mg^{2+} effect on the phosphorylation state of $KaiC^{E487A}$, $KaiC^{R488A}$, and $KaiC^{T495A}$, we added excess amount (20 mM, four times higher than the regular concentration) of Mg^{2+} in the reaction mixture. Because its high concentration induces the dephosphorylation of KaiC (Jeong et al., 2019), we expected that Mg^{2+} will attenuate the kinase activity of the hyperphosphorylated KaiC mutants ($KaiC^{E487A}$ and $KaiC^{T495A}$) and lead to some degree of dephosphorylation. The effect was not observed for $KaiC^{E487A}$ with 20 mM Mg^{2+} (Figure 4.3D). However, $KaiC^{T495A}$ showed dephosphorylation in the beginning and remained for 48 hours at ≈75% phosphorylation level (Figure 4.3E), which is ≈20% lower than that of the regular condition (5 mM Mg^{2+}). In the case of $KaiC^{R488A}$, the dephosphorylation was slightly enhanced by higher Mg^{2+} at the beginning but stopped at the same phosphorylation level (≈50% phosphorylation) after 12 hours (Figure 4.3F), in a similar manner as that of the regular condition (5 mM Mg^{2+}).

In sum, higher Mg^{2+} concentration enhanced the dephosphorylation of $KaiC^{T495A}$ and $KaiC^{R488A}$ but its effect on $KaiC^{E487A}$ was miniscule. We previously suggested that the dephosphorylation is induced when Mg^{2+} is bound in the active site and its affinity is increased or decreased with the buried or exposed conformation of A-loop, respectively (Jeong et al., 2019). Therefore, the dynamic equilibrium of A-loop conformations can be

predicted based on phosphorylation levels of the KaiC mutants. For $KaiC^{E487A}$, the equilibrium cannot be shifted toward the buried conformation even at high Mg^{2+} concentration (Figure B.4) because severing the seemingly strong glutamate H-bond exposes the A-loop by making it irreversibly flexible, up to a level that is unperturbed by Mg^{2+}'s presence (Tseng et al., 2014). On the other hand, for $KaiC^{T495A}$, the A-loop's dynamic equilibrium partially shifted toward the buried conformation, with which more abundant Mg^{2+} has a better chance at binding KaiC and activating dephosphorylation, following the Le Chatelier's principle (Figure B.4). The dynamic equilibrium seems balanced in $KaiC^{R488A}$, since its phosphorylation level stagnated at ≈50%.

4.2.3 Decreasing adenosine triphosphate (ATP) ratio enhanced the KaiC dephosphorylation

Decreasing ATP or increasing adenosine diphosphate (ADP) ratio in the nucleotides pool can also induce the dephosphorylation of KaiC. A temporary drop in the ATP ratio to 50% during the phosphorylation phase is known to induce dephosphorylation (Rust et al., 2011). Unlike Mg^{2+}, ATP and ADP are used not as regulators but as reactants for phosphorylation and dephosphorylation reactions (Egli et al., 2012; Jeong et al., 2019; Nishiwaki & Kondo, 2012). We investigated the ATP ratio effect on the KaiC phosphorylation with $KaiC^{E487A}$, $KaiC^{R488A}$, and $KaiC^{T495A}$. The KaiC mutants were dephosphorylated with increasing ADP, in a similar manner as that of increasing Mg^{2+} concentration (Figure 4.3G, H, and I). Because ATP and ADP are reactants in the phosphorylation and dephosphorylation reaction of KaiC, adding ADP cannot directly shift the dynamic equilibrium of A-loop conformation (Figure B.5). However, phosphorylation is inhibited when ADP is bound to the CII domain of KaiC, even when

the A-loop's conformation is exposed; conversely if ADP binds to KaiC when the A-loop is buried, dephosphorylation will proceed (Egli et al., 2012).

Based on the results of the mutation studies, we can predict how much of each A-loop conformation is favored in the dynamic equilibrium for the KaiC mutants. The A-loop of $KaiC^{E487A}$ seems to constantly stay exposed, since the presence of ADP was not able to induce dephosphorylation. However, $KaiC^{E495A}$ and $KaiC^{R488A}$ have the dynamic equilibrium slightly favored toward the buried state, although the former's case was less so. Therefore, the H-bond of E487 would be the most determinant and of R488 would be the least so at stabilizing the buried conformation of the A-loop.

4.2.4 KaiB attenuates the phosphorylation activated by breaking the H-bonds in A-loop

Traditionally, KaiB is known to indirectly induce the dephosphorylation of KaiC by sequestering KaiA from the A-loop (Chang et al., 2015; Qin, Byrne, Mori, et al., 2010; Tseng et al., 2014). Because no direct effect of KaiB on the KaiC phosphorylation has been reported, we used the KaiC mutants that remain constitutively hyperphosphorylated in the absence of KaiA to examine the effect. When KaiB was added into the reaction mixtures containing only the KaiC mutants, all of them showed dephosphorylation to a certain degree. Interestingly, $KaiC^{E487A}$, which was unable to be dephosphorylated with other treatments, showed dephosphorylation in the presence of KaiB (Figure 4.4A). $KaiC^{T495A}$ displayed the largest effect among the mutants (≈20%), although the magnitude was smaller than that of the KaiC wild-type (Figure 4.4B). $KaiC^{R488A}$ also showed ≈10% more dephosphorylation in the presence of KaiB (Figure 4.4C). Because the phosphorylation and dephosphorylation are determined by the A-

loop conformation, adding KaiB must induce dephosphorylation on the KaiC mutants by shifting the dynamic equilibrium toward the buried conformation (Figure B.2).

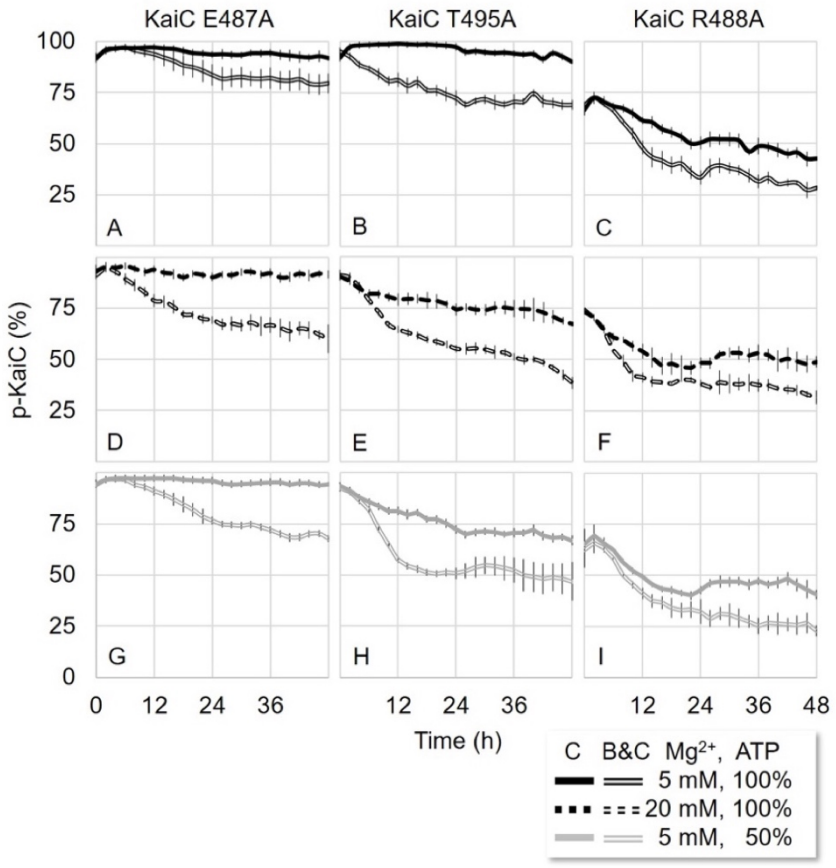

Figure 4.4 KaiB binding locks the buried conformation of A-loop inducing the dephosphorylation of KaiC mutants. (A-I) All are the same as Figure 4.3 except adding KaiB (3.4 μM) in the reaction mixture.
Source: P. Kim et al., Submitted

We also examined the Mg^{2+} effect in the presence of KaiB. Adding Mg^{2+} enhanced the dephosphorylation in all KaiC mutants in the presence of KaiB (Figure 4.4D-F). High Mg^{2+} concentration shifts the dynamic equilibrium more toward the buried conformation, an effect additive to the KaiB effect. It is also worth noting that $KaiC^{E487A}$ which seemed impossible to dephosphorylate underwent dephosphorylation and became responsive to ADP and Mg^{2+} only when KaiB is present (2A, 2D, 2G).

Increasing the ADP ratio also induced further dephosphorylation of KaiC^{T495A} and KaiC^{R488A} in the presence of KaiB (Figure 4.4G-I). Therefore, KaiB binding shifts the dynamic equilibrium toward the buried conformation, even on KaiC^{E487A}, which was unable to shift the equilibrium with any other treatments.

Based on the observation, KaiB directly induces the dephosphorylation of KaiC through at least one additional mechanism other than the sequestration of KaiA, which is an indirect effect. These two functional properties of KaiB may bring about a synergetic effect on the dephosphorylation of KaiC at the onset of the dephosphorylation phase, contributing to making the oscillation more robust.

4.2.5 CI flexibility governs the damped oscillatory phosphorylation in KaiC^{E488A}

The phosphorylation profile of KaiC^{R488A} is the most intriguing because of its balance between spontaneous phosphorylation and dephosphorylation: remaining phosphorylated for the first 2 hours and reaching a steady-state, mildly elevated (≈50%) level (Figure 4.3C). It seems to have the characteristic of the damped oscillator for the KaiC^{E488A} alone reaction. We previously reported that changing the Mg^{2+} concentration in the reaction mixture modulates the phosphorylation and dephosphorylation of KaiC (Jeong et al., 2019). It seems if we decrease the Mg^{2+} concentration, we may observe the higher (or longer) phosphorylation state for KaiC^{R488A} alone reaction. To test the Mg^{2+} effect on the phosphorylation of KaiC^{R488A}, we monitored the phosphorylation states in different Mg^{2+} concentrations in the absence or presence of KaiB. KaiC^{R488A}'s unusual balance between the two antagonistic reactions renders it with a unique phosphorylation pattern. At low Mg^{2+} concentration (1 mM), KaiC^{R488A} distinctively showed kinase activity for 12-h and underwent dephosphorylation afterwards in the KaiC^{R488A} alone

reaction mixture (Figure 4.5A). When KaiB is present in the reaction mixture, dephosphorylation started earlier than when it is absent (Figure 4.5B). This abnormal behavior could come from the flexibility change on the CII domain of KaiC throughout the phosphorylation state (Chang, Kuo, Tseng, & LiWang, 2011). As hypophosphorylated KaiC becomes fully phosphorylated, the CII domain rigidifies, and the A-loop's dynamic equilibrium shifts from the exposed to the buried conformation (Figure B.6). Therefore, $KaiC^{R488A}$ autophosphorylates initially (phosphorylation phase) because the A-loop is exposed in the flexible CII domain. As KaiC gradually becomes fully phosphorylated, the CII domain rigidifies and the A-loop prefers the buried conformation, eventually inducing dephosphorylation (Figure B.7).

The binary KaiC-KaiB complexation seems to affect the KaiC mutants in an irreversible manner unlike that of ADP or Mg^{2+}, as both $KaiC^{E487A}$ and $KaiC^{R488A}$ consequently showed a higher degree of dephosphorylation when KaiB was present. This bolsters the notion that KaiC-KaiB binding locks the rigid CII domain and eventually shifts the conformational equilibrium of A-loop toward its buried state. KaiB's binding KaiC and inducing the A-loop burial would ensure dephosphorylation to take place at the correct phase of the clock and the biological timekeeping to run clockwise.

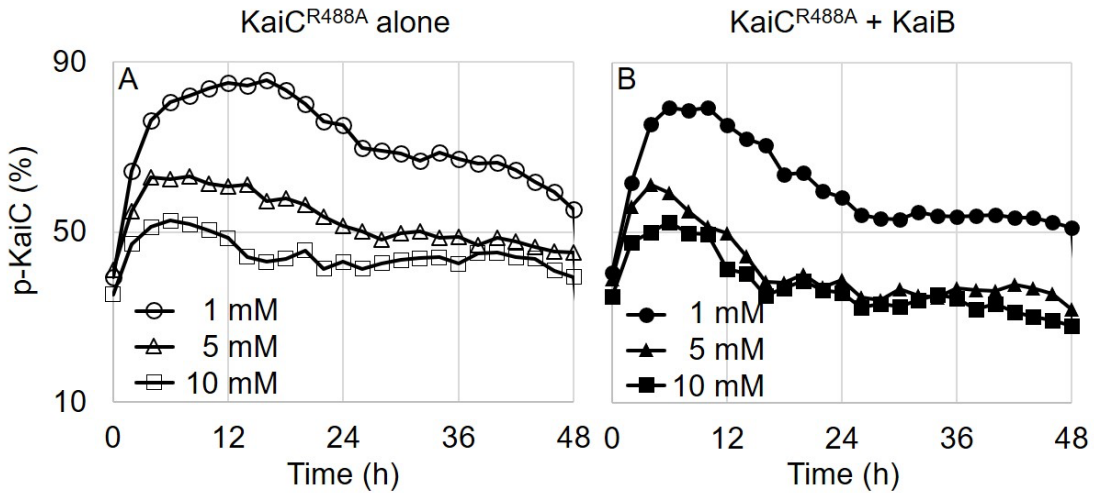

Figure 4.5 The spontaneous phosphorylation and dephosphorylation of KaiC^{R488A}. The phosphorylation state of KaiC^{R488A} was measured without KaiA and KaiB every 2-hour for 2 days. The Mg^{2+} concentration of each reaction was labeled on the graph (A). The phosphorylation state of KaiC^{R488A} in the presence of KaiB (B).
Source: P. Kim et al., Submitted

4.3 Discussion

The cyanobacterial circadian oscillator shows an oscillatory phosphorylation and dephosphorylation with ≈24-h period. To induce autophosphorylation or autodephosphorylation of KaiC, the A-loop conformation's stabilization in the exposed or buried conformation leads to phosphorylation or dephosphorylation, respectively. Various interactions among the Kai proteins sequentially regulates the A-loop's conformation to generate an oscillatory KaiC phosphorylation and dephosphorylation. When KaiC is unphosphorylated, KaiA binding to the A-loop shifts the dynamic equilibrium toward the exposed conformation, which activates the KaiC phosphorylation. By breaking the inter- and intra-subunit H-bonds on A-loop, KaiC can be phosphorylated without KaiA. When KaiC is fully phosphorylated, KaiB binds to KaiC and sequesters KaiA from the A-loop. The dissociation of KaiA shifts the dynamic equilibrium toward the buried conformation, which induces the dephosphorylation of

KaiC.

However, a significant amount of free KaiA proteins are still present in the reaction mixture when KaiC is ready to start the dephosphorylation phase (Hong et al., 2020; Qin, Byrne, Mori, et al., 2010). A decrease in free KaiA due to its sequestration by KaiB would not necessarily reverse the kinase reaction; rather, it would just slow down the kinase reaction (Nakajima, Ito, & Kondo, 2010; Rust et al., 2011). In other words, with a lower number of active KaiA in the mixture the level of phosphorylated KaiC would increase slowly, but its reduction would not trigger dephosphorylation. Therefore, the sequestration of KaiA alone is not enough to fully explain the transition and the oscillator's clockwise sequential phosphorylation and dephosphorylation (Chang et al., 2011; Nishiwaki et al., 2007; Rust et al., 2007). Here, we found the additional functionality of KaiB that plays a key role in the transition between the KaiC phosphorylation and dephosphorylation phases.

Introducing KaiB's novel function, we propose a detailed mechanism of the circadian oscillation in the mechanistic level (Figure 4.6). When KaiC is in the unphosphorylated state (U), the CII domain remains flexible and the dynamic equilibrium of A-loop conformation shifts toward the exposed (Chang et al., 2011). KaiA binds the exposed A-loop and KaiC phosphorylates itself until it is fully phosphorylated (Y. I. Kim et al., 2008; Vakonakis & LiWang, 2004) (U → T → ST). When the KaiC phosphorylation peaks (ST), its CII domain becomes rigid and is stacked on the CI domain (Chang et al., 2011). This conformational change shifts the A-loop's dynamic equilibrium toward the buried conformation and KaiC starts to dephosphorylate. KaiB binds to the CI domain of KaiC and locks the conformation

continuing dephosphorylation (ST → S → U). Although a significant amount of free KaiA is present in the oscillatory reaction mixture at this point, the locked conformation does not allow KaiA from binding the A-loop. When KaiC is unphosphorylated (U), KaiB dissociation allows the CII domain to be conformationally flexible and KaiC starts the phosphorylation cycle again (U → T → ST).

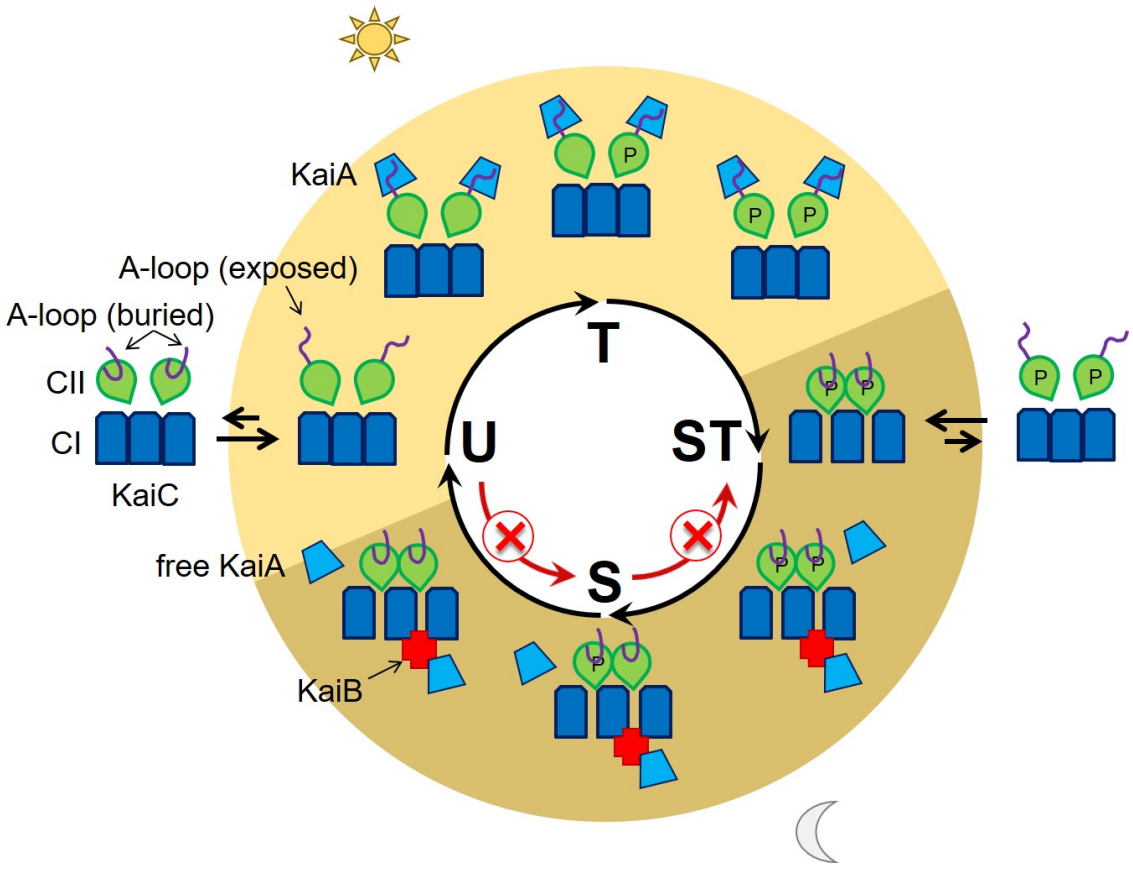

Figure 4.6 The mechanistic model of the circadian oscillator in cyanobacteria. To initiate the dephosphorylation, A-loop is buried conformation in the rigid CII domain (ST). KaiB binding to CI domain locks the buried conformation to keep the dephosphorylation of KaiC. The major phosphorylation states of KaiC were written on the white circle. The protein interactions corresponding to the phosphorylation states are shown on the colored (light and dark yellow) circle. To simplify, only three subunits of CI domain and two subunits of CII domain were drawn.
Source: P. Kim et al., Submitted

To mimic hypophosphorylated (U) and hyperphosphorylated (ST) KaiC, alanine ($KaiC^{AA}$) and glutamate ($KaiC^{EE}$) substitutions are applied respectively to both phosphorylation sites—S431 and T432 (Ito et al., 2007; Kitayama et al., 2008). Surprisingly, previously reported fluorescence anisotropic data suggest that $KaiC^{EE}$ has a greater affinity for KaiA than $KaiC^{AA}$, in the absence of KaiB(Qin, Byrne, Mori, et al., 2010). It means that the free KaiA proteins can bind to A-loop of ST-KaiC and inhibit the dephosphorylation (ST → S) and stay on the hyperphosphorylated KaiC. Then, KaiB's role of locking the rigid conformation of CII domain in KaiC becomes even more crucial when it comes to maintaining the phosphatase activity at the beginning of the dephosphorylation phase (ST → S), considering that there still is residual free KaiA in the mixture enough to offset dephosphorylation. KaiA's differential affinity to KaiC has previously been reported, and it was argued that it depends on the phosphorylation state of KaiC; this ensures that the oscillator runs clockwise during the phosphorylating phase (Mori et al., 2018; Qin, Byrne, Xu, Mori, & Johnson, 2010). However, the use of phosphomimetics only provides a partial understanding of the dynamic behaviors of A-loop, KaiC, and its kinase and phosphatase activities, leaving it difficult to pinpoint the cause and effect of the post-translational modification. Our finding here adds another factor that contributes to the clockwise "ticking": KaiB's binding KaiC allosterically induces the conformational burial of the A-loop, shifting the equilibrium towards the dephosphorylation phase.

Among many targets, the hyperphosphorylated KaiC-KaiB complex in *S. elongatus* suppresses *kaiBC* transcription. The resultant reduction in KaiC and KaiB concentrations creates a transcription-translation feedback loop (TTFL), ensuring that

their production peaks only when unphosphorylated KaiC dominates at dawn. The hallmark of KaiABC-based post-translational oscillator (PTO) is that it can withstand significant cellular noise coming from various sources, including variations in the abundance of clock components (Tomita et al., 2005). Overexpression of KaiA induces the constitutive phosphorylation of KaiC and causes the oscillation to dampen, a pattern observed in TTFL-based KaiBC hourglass models in other organisms.

Among the central oscillator components, *kaiC* is thought to be the oldest, while *kaiA* being the youngest (V. Dvornyk et al., 2003). Thus, it is suggested that the emergence of two-component KaiBC timekeeper—a supposed relic of the past that gave rise to today's intricate cyanobacterial timekeeper—might have preceded that of *bona fide* KaiABC circadian clock (Johnson et al., 2017). By adjusting the H-bonding network on the A-loop, we succeeded in shifting the equilibrium between the two antagonistic reactions sustaining the phosphorylation level of KaiC at various levels without the presence of KaiA, a possible feature of the KaiBC timekeeping system. In addition, $KaiC^{R488A}$'s partial responsiveness to various cues and eventual return to its initial phosphorylation level hints at the potential mechanism of a damped oscillator, a possible intermediate step in the development of the timekeeper (Johnson et al., 2017). The fact that the primary sequences of the A-loop vary between different *kaiC*-harboring species yet the general motifs of *kaiC* are conserved brings our attention to the importance of the A-loop as the master regulator of post-translational oscillator (Axmann, Hertel, Wiegard, Dorrich, & Wilde, 2014; Ma, Mori, Zhao, Thiel, & Johnson, 2016).

Previously, we argued that a KaiC-alone hourglass can oscillate under the alternating Mg^{2+} concentration *in vitro*, and this perhaps puts the emergence of Mg^{2+} homeostasis after that of the primeval timekeeper on the clock's evolutionary timeline (Jeong et al., 2019). Since the endogenous Mg^{2+} concentration was reported to remain constant in *S. elongatus* (P. Kim, Porr, et al., 2020), the emergence of a damped oscillator as a better timekeeping system than the cue-dependent hourglass fits well into the picture (Johnson et al., 2017). After going through multiple evolutionary steps, the current self-sustained circadian oscillator has emerged as a biologically efficient way to exploit the periodic availability of solar energy.

The unidirectionality of sequential KaiC phosphorylation to run clockwise and the KaiC-KaiB complexation that takes place only at the correct phase tunes the timing of bifunctional CikA's binding and its possible inactivation by oxidized quinone, which causes the phase of KaiC phosphorylation rhythm to delay in response to a dark pulse application when applied in the falling phase of the clock (Kiyohara et al., 2005). KaiB binding's allosteric induction of A-loop burial also has a potential role in the entrainment process, since maintaining the A-loop's buried conformation during the falling phase of the clock is crucial not only for the maintaining the KaiC-KaiB-CikA complex, but also in that KaiA cannot tether the A-loop in its exposed conformation and run the rhythm backward—toward phosphorylation. If the A-loop becomes exposed at this stage, KaiA rather than CikA can be inactivated by oxidized quinone, which would advance the phase instead of delaying it (M. Kaur et al., 2019; P. Kim, Porr, et al., 2020). It is through this process that KaiB initiates the dephosphorylation phase at the correct timing of day and ensures that CikA's binding takes place accordingly.

If the proliferation of cyanobacteria billions of years ago led to the Great Oxygenation that transformed Earth's anoxic atmosphere, bioengineering cyanobacteria can be considered as one of the potential strategies to combat environmental and energy crises. By understanding the functional and structural properties of the cyanobacterial circadian clock, we could bring the hope of undoing the man-made production of carbon dioxide closer to reality.

CHAPTER 5

CONCLUSION

To understand better the role of KaiC in the cyanobacterial circadian clock, an extremely high degree of protein purity is necessary to reconstitute the *in vitro* oscillations, as demonstrated in the first part of this research. For other related areas of *in vitro* research, which are vital for studying the function, structure, and interactions of a protein of interest, this methodology may help improve what is normally a laborious process into a faster and cost-effective protocol that can serve as a basis for protein purification and the temporal detection of post-translational modification.

After we have established the period retaining effect of maintaining the summed concentration of KaiA and CikA to 1.2 μM, the long-delayed *in vitro* quinone entrainment study was resumed (P. Kim, Porr, et al., 2020). 0.6 μM CikA and 0.6 μM KaiA produced statistically meaningful period retention but the magnitude of phase shift was downgraded overall compared to that of *in vivo*. Thus, we reasoned that the overall delayed phase might be due to too much CikA in the mixture and settled with 0.3 μM CikA and 0.9 μM KaiA for the quinone entrainment. The 4-h application of oxidized Q_0 at CT 8 generated a 7-h phase advance and at CT 22 a 4-h phase delay, a pattern in consonance with the PRC of *in vivo* 4-dark pulse application (Figure 5.1).

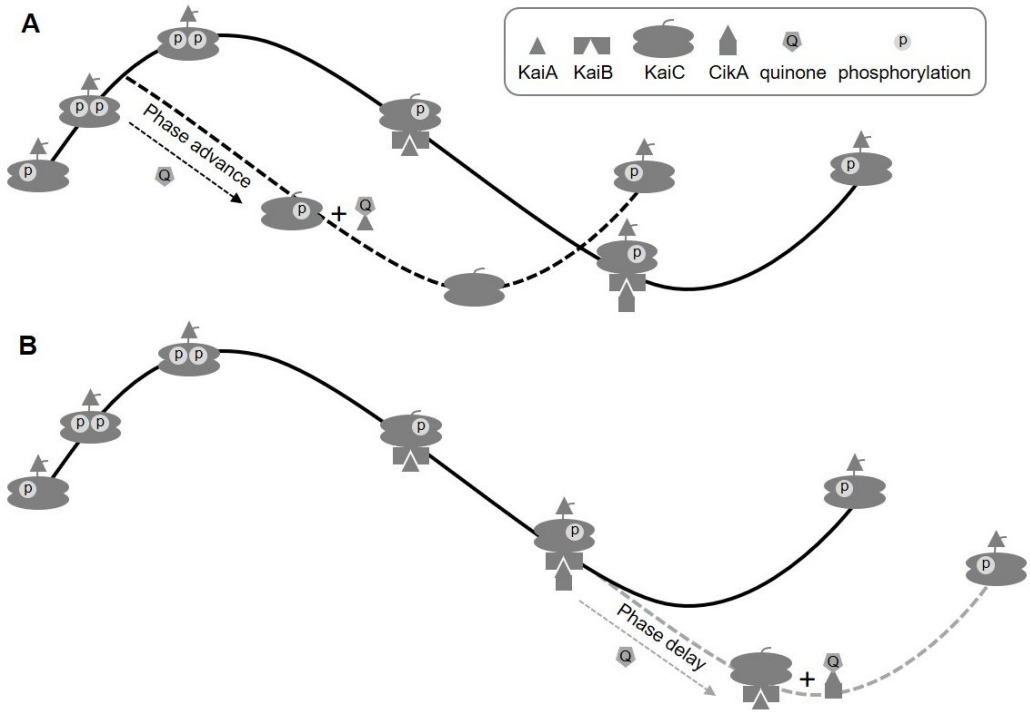

Figure 5.1 The entraining mechanism of the cyanobacterial circadian clock with oxidized quinone. The circadian oscillation without or with entrainment are on the solid or dotted line, respectively. The phosphorylation on the right and the left in KaiC represent amino acid residues S431 and T432, respectively. (A) The mechanism of phase advance. When oxidized quinone is applied on the phosphorylation phase, KaiA dissociates from the A-loop by binding oxidized quinone. The dissociation of KaiA brings early dephosphorylation of KaiC resulted in the phase advance (black dotted line). (B) The mechanism of phase delay. When oxidized quinone is applied in the dephosphorylation phase, CikA dissociates from KaiB by binding oxidized quinone and KaiA binds to KaiB. This binding extends dephosphorylation of KaiC for a while and resulted in the phase delay (gray dotted line).
Source: P. Kim, Porr, et al., 2020

Therefore, it was finally established that CikA plays a role in generating a phase delay in response to oxidized quinone *in vitro*. Here we introduce the theoretical mechanism behind the phase shifts generated by temporal quinone inactivation of KaiA and CikA. In KaiC's autokinase mode, the binary KaiA-KaiC complex dominates. The addition of oxidized quinone at this particular moment can inactivate KaiA, and a temporary decrease in active KaiA concentration leads to premature dephosphorylation of KaiC, leading to a phase advance (Figure 5.1). In a different scenario, after complete

phosphorylation is achieved by KaiC, its affinity for KaiB increases. The binary KaiC-KaiB complex exposes a binding site on KaiB where both KaiA and CikA can bind. CikA will compete with KaiA for the binding, and this would lead to a rise in free KaiA that has been outcompeted by CikA. The competition gives CikA an upper hand since KaiB is its only binding site as compared to KaiA's more promiscuous binding to both KaiB and the A-loop of KaiC. Then, the hypothetical quaternary KaiA-KaiC-KaiB-CikA complex forms, and adding oxidized quinone would disable CikA and force it to dissociate from the complex, finally leaving the spot open for KaiA to be sequestered (Figure 5.1). The resultant drop in free KaiA extends the dephosphorylating phase, causing the observed phase delay.

It is also worth noting that phase delay would not be generated without CikA in the mixture, since the only component that responds to oxidized quinone would be KaiA, of which its stimulatory effect is prominent only during the KaiC phosphorylation phase. KaiA is known to have relatively similar affinities for various phospho-forms of KaiC (Kageyama et al., 2006), while KaiB binds preferentially to the S431-phosphorylated form (Nishiwaki et al., 2007; Rust et al., 2007). This means that CikA's presence in the mixture frees up more KaiA from KaiB, yet CikA's time frame in delaying the phase in response to quinone is confined only to the dephosphorylation phase after its full phosphorylation. In sum, CikA's metabolite-sensing, clock-resetting ability, competition with KaiA, and modulation of KaiC phosphorylation rhythm support its role in the input pathway. In a more realistic situation, the solar light intensity becomes lower during the day (on a cloudy day); surprisingly, the expression of dusk genes peaks earlier (Piechura, Amarnath, & O'Shea, 2017). KaiA and CikA that

respond to oxidized quinone, which can become available at any time during the day depending on the occasionally irregular timing of darkness, render cyanobacteria with the ability to advance or delay the KaiC phosphorylation cycle and thus its gene expression, flexibly orchestrating its metabolic rhythm to fit the environmental alterations. In conjunction with ATP/ADP entrainment, the quinone entrainment system synergistically contributes to the robustness of the circadian oscillations.

The rate-limiting step of our *in vitro* studies lies in the lack of structural data. More specifically, in addition to CikA's and KaiA's response to quinone analogs DBMIB and Q_0, what kind of quinone actually binds them in *S. elongatus* has remained elusive, considering there are different types (besides the most biologically abundant, PQ) in cyanobacteria. Although it is easier said than done, the protein structure of full-length CikA would be of tremendous help in analyzing its functionally enigmatic nature. In concert with ATP/ADP sensing by KaiC, at what degree quinone sensing actually synchronizes the circadian clock and how biologically relevant this mechanism are also worthy questions ahead of us.

What further complicates the picture is that CikA is implicated in the output pathway as a phosphatase against phosphorylated RpaA (Gutu & O'Shea, 2013). CikA's seemingly multifaceted role as both input and output stems from its involvement in the negative feedback mechanism, as *ΔcikA* displays heightened overall gene expression level (Taniguchi, Takai, Katayama, Kondo, & Oyama, 2010). In addition, the presence of a histidine kinase domain in CikA suggests its potential involvement in the two-component phosphate transfer reaction, meaning that there could be a possible receiver domain in the output pathway, such as RpaA. The ongoing controversy surrounding

CikA's true role in the cyanobacterial clock constantly reminds us that our goal is to fully delineate the nature of CikA through the addition of output pathway components *in vitro*.

Then, how is information about metabolite and ion abundances as proxies for light and darkness passed down to the prokaryotic circadian pacemakers? Questions still loom as we have just embarked on this journey, but it was these very questions that initially drove us to search for more answers. Through KaiA's binding and exposing the A-loop of KaiC, KaiC-bound Mg^{2+} becomes loosened and released, and KaiC's unbound catalytic base swings toward the ATP molecule, commencing autophosphorylation. Quinone's inactivation of KaiA and CikA can advance and delay the phase of oscillation respectively, depending on the timing of dark-induced quinone abundance. Hopefully, our continuous effort to reconstitute the *in vitro* circadian clock will pave the way to tackle the remaining uncertainties; the introduction of quinone and CikA to the mixture and elucidation of the role of Mg^{2+} are only the beginning of our ultimate goal of accurately representing the entire circadian clock in a test tube. One day, a stroke of insight coming from Takao Kondo's laboratory introduced the idea of reanimating the post-translational circadian oscillator by mixing the Kai proteins and Mg^{2+} in a test tube; coincidentally in the same year, KaiA's and CikA's quinone-sensing ability was discovered. Probably no one expected these seemingly disparate topics to eventually converge into today's expanded mixture, a powerful tool that can guide us through the functional details of the proteinaceous clock at a molecular level. Having inhabited billions of years on Earth, perhaps cyanobacteria has been right all along: life is all about timing.

APPENDIX A

SUPPLEMENTARY MATERIALS FOR CHAPTER 3

This appendix lists the tables and figures that are supplementary to CHAPTER 3, CikA, an Input Pathway Component, Senses the Oxidized Quinone Signal to Generate Phase Delays in the Cyanobacterial Circadian Clock.

Table A.1 Statistical Analysis of the Period

KaiA Conc. (μM)	CikA Conc. (μM)	Period (h) Exp. 1	Period (h) Exp. 2	Period (h) Exp. 3	Average (h)	Standard Deviation (h)	p-value
1.2	0	20.54	21.85	23.53	21.97	1.50	
	0.3	20.19	22.39	21.88	21.49	1.15	0.9396
	0.6	19.87	21.37	21.56	20.93	0.93	0.5753
	0.9	19.87	21.3	20.85	20.67	0.73	0.3983
	1.2	19.29	20.61	20.07	19.99	0.66	0.1224
0.9	0	21.53	23.00	21.00	21.84	1.04	
	0.3	20.59	21.80	20.25	20.88	0.81	0.4865
	0.6	20.01	21.03	19.64	20.23	0.72	0.1291
	0.9	19.43	20.74	19.13	19.77	0.86	0.0447
	1.2	19.00	20.54	19.17	19.57	0.84	0.0284
0.6	0	23.17	21.79	22.34	22.43	0.69	
	0.3	20.84	20.64	21.27	20.92	0.32	0.00172
	0.6	20.44	20.28	20.49	20.40	0.11	0.00021
	0.9	19.82	19.78	19.72	19.77	0.05	5.4e-05
	1.2	18.86	19.39	19.13	19.13	0.27	5.2e-08

Source: P. Kim, Porr, et al., 2020

Table A.2 Periods of the KaiC Phosphorylation at Different Temperatures

Temp.(°C)	Period (h)	Period (h)	Period (h)	Average (h)	Standard Deviation (h)
35	19.29	20.5	19.4	19.73	0.67
30	20.44	20.28	20.49	20.4	0.11
25	20.75	21.43	20.12	20.77	0.66

Source: P. Kim, Porr, et al., 2020

Table A.3 Statistical Analysis of the Period at Different Temperatures Using the Tukey HSD Method

Temp. (°C)	p-value
30 vs. 25	0.7068
30 vs. 35	0.1264
25 vs. 35	0.3493

Source: P. Kim, Porr, et al., 2020

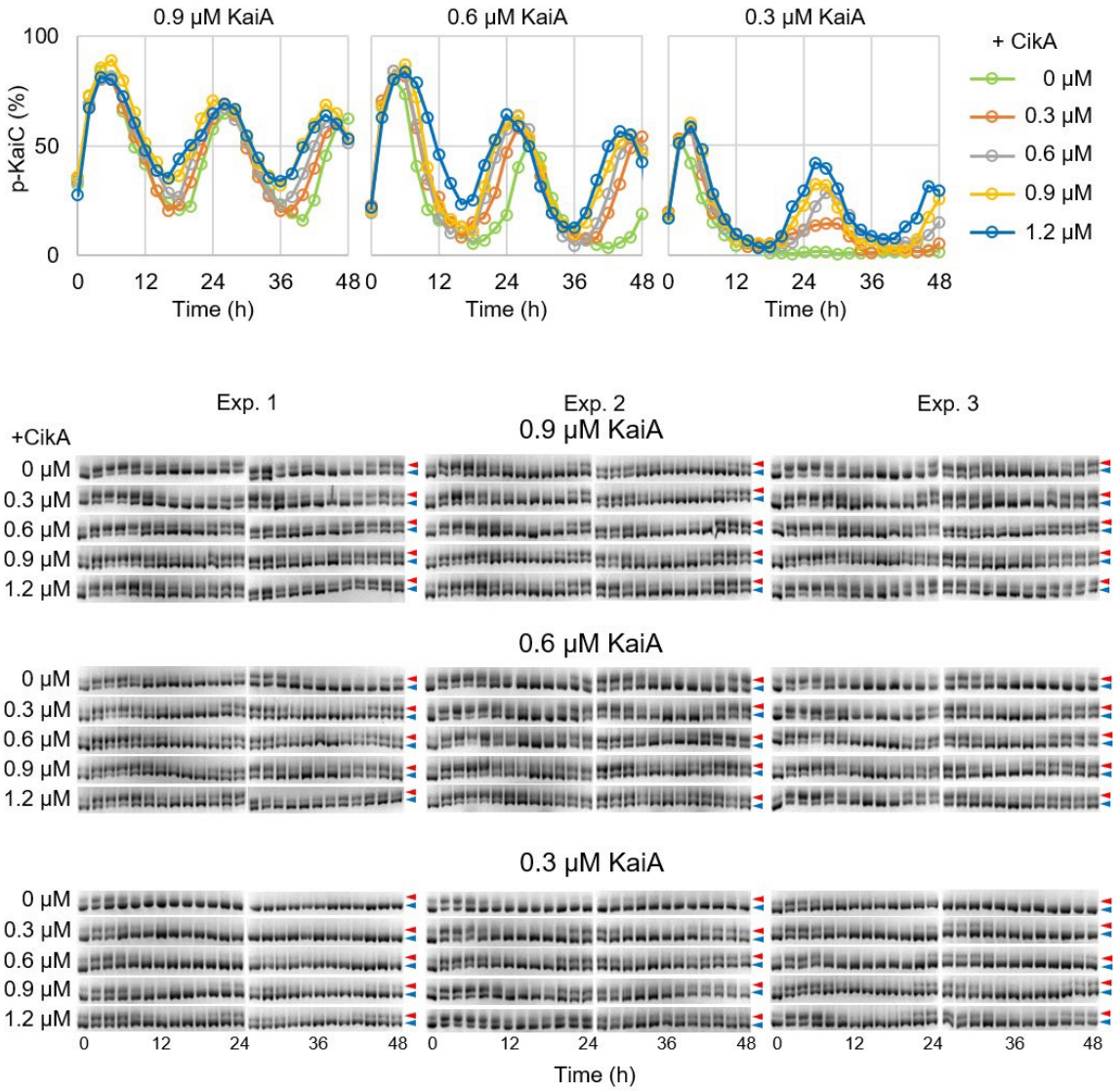

Figure A.1 KaiC phosphorylation with various KaiA and CikA concentrations. The three independent replicates are labeled with Exp. 1, Exp. 2, and Exp. 3. The densitometry graphs of Exp.1 are shown on the top panel. KaiA concentrations for the oscillation mixtures are shown on the center of the gel pictures. The phosphorylated (red triangle) and unphosphorylated (blue triangle) KaiC bands are separated by the 6.5% SDS-PAGE. *Source: P. Kim, Porr, et al., 2020*

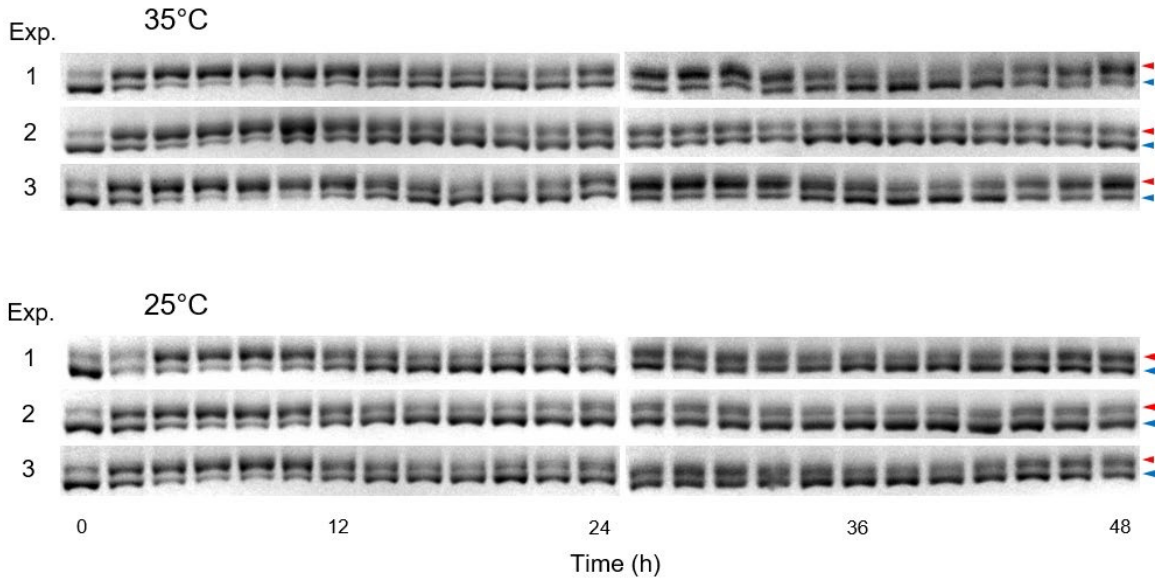

Figure A.2 SDS-PAGE for Figure 3.3 and Table A.2. The three independent replicates are labeled with Exp. 1, Exp. 2, and Exp. 3. The densitometry graphs of Exp.1 are shown on the Figure 3.3A in the main text. The phosphorylated (red triangle) and unphosphorylated (blue triangle) KaiC bands are separated by the 6.5% SDS-PAGE. *Source: P. Kim, Porr, et al., 2020*

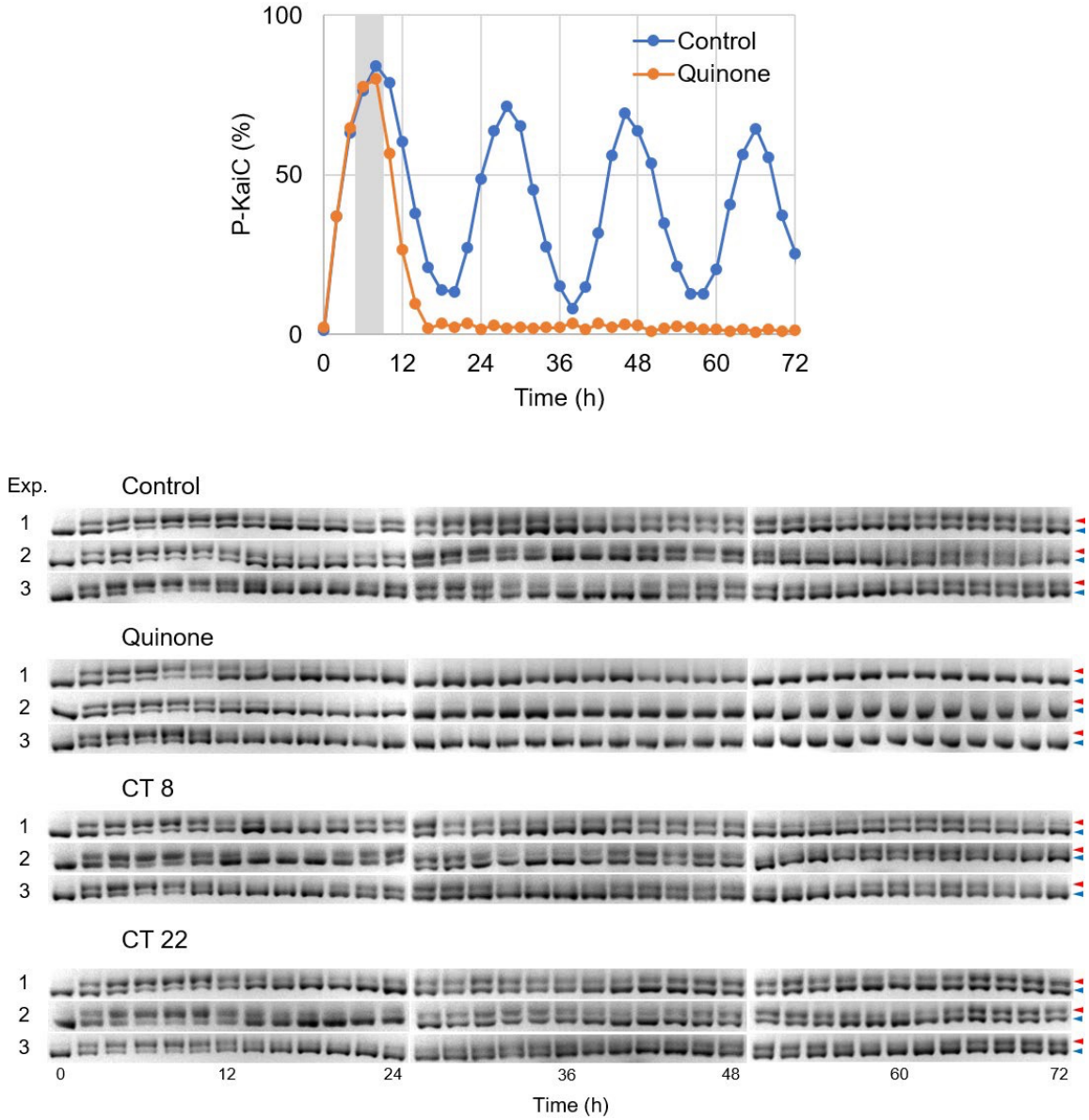

Figure A.3 Suppression of KaiC phosphorylation by quinone. The three independent replicates are labeled with Exp. 1, Exp. 2, and Exp. 3. The densitometry graphs of Exp.1 are shown on the Figure 3.4A and 3.4B in the main text and the top panel in this figure. The phosphorylated (red triangle) and unphosphorylated (blue triangle) KaiC bands are separated by the 6.5% SDS- PAGE. KaiA (0.6 μM), KaiB (3.4 μM), KaiC (3.4 μM), and CikA (0.6 μM) are mixed to generate circadian oscillation and treated with oxidized quinone to generate the phase change.
Source: P. Kim, Porr, et al., 2020

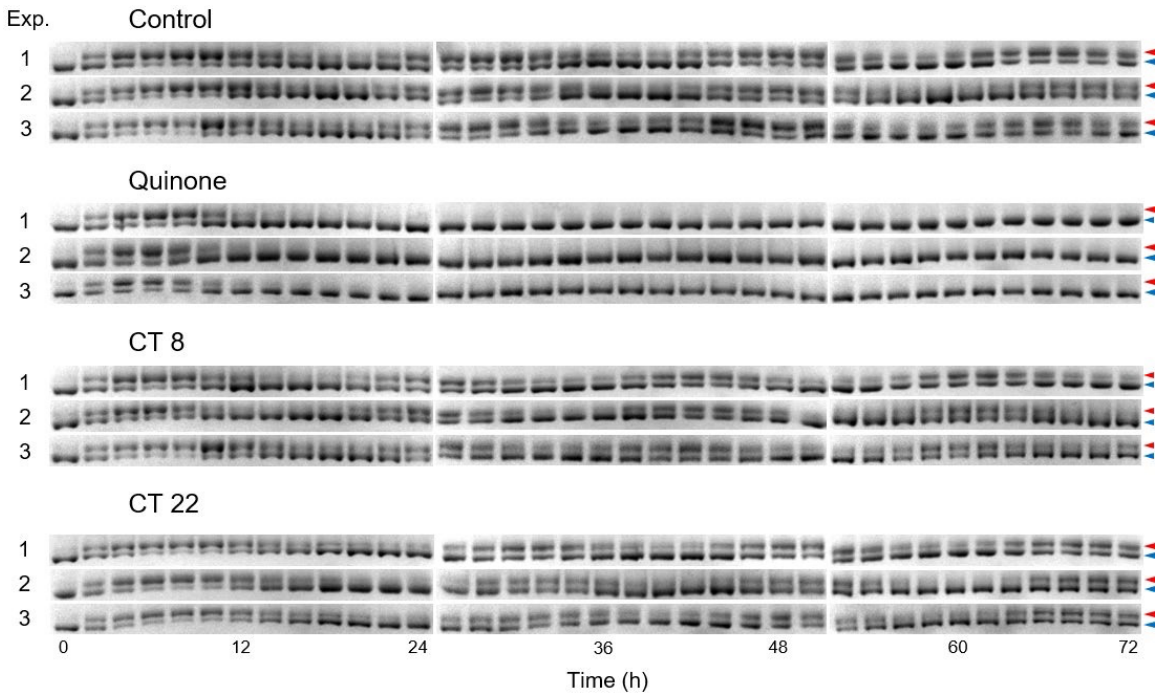

Figure A.4 Resetting circadian clock *in vitro* with oxidized quinone. The three independent replicates are labeled with Exp. 1, Exp. 2, and Exp. 3. The densitometry graphs of Exp.1 are shown on the Figure 3.4A and 3.4B in the main text and the top panel in this figure. The phosphorylated (red triangle) and unphosphorylated (blue triangle) KaiC bands are separated by the 6.5% SDS-PAGE. KaiA (0.9 μM), KaiB (3.4 μM), KaiC (3.4 μM), and CikA (0.3 μM) are mixed to generate circadian oscillation and treated with oxidized quinone to generate the phase change.
Source: P. Kim, Porr, et al., 2020

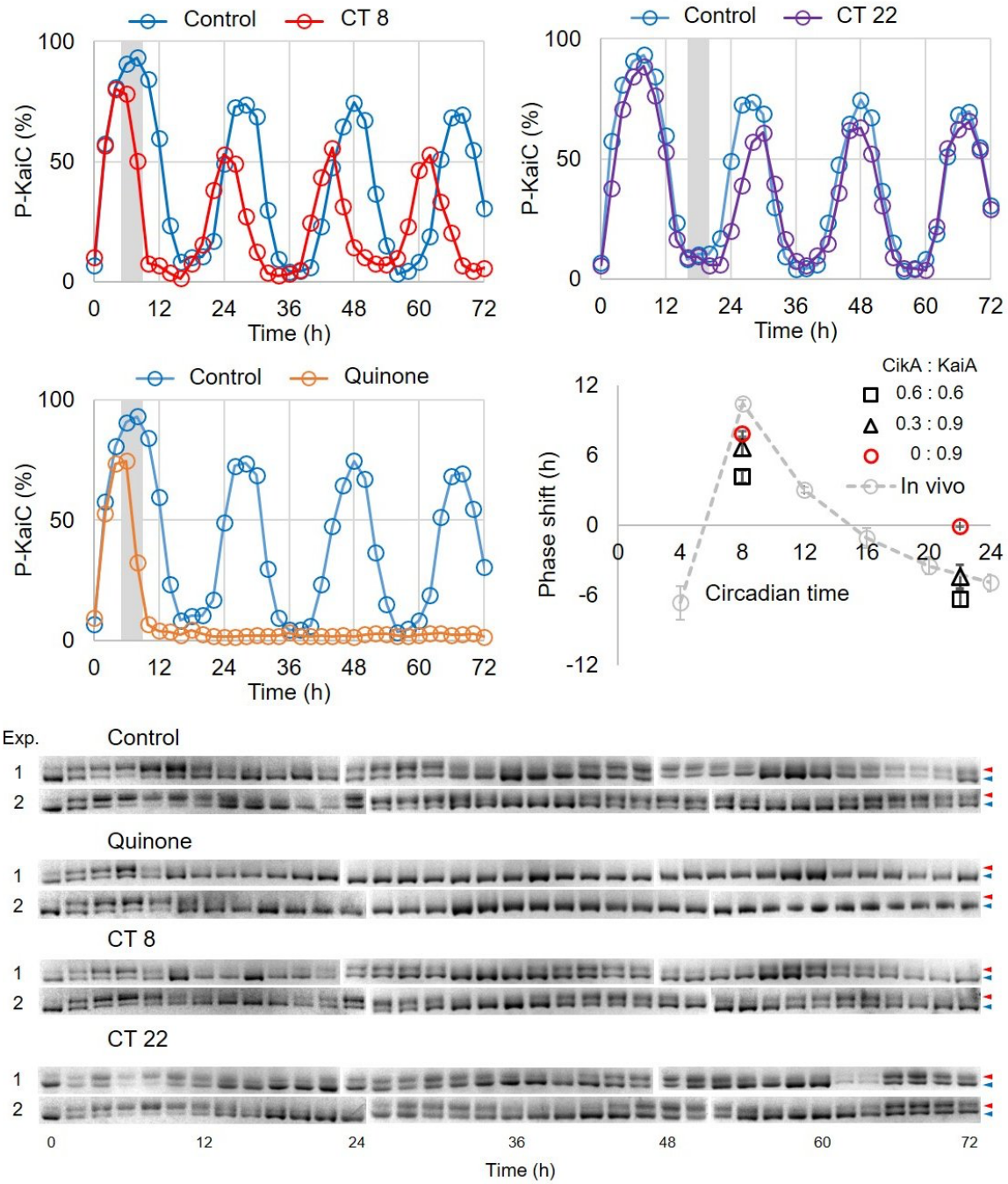

Figure A.5 Resetting circadian oscillator *in vitro* with oxidized quinone. The two independent replicates are labeled with Exp. 1 and Exp. 2. The densitometry graphs of Exp.1 are shown on the upper panels in this figure. The phosphorylated (red triangle) and unphosphorylated (blue triangle) KaiC bands are separated by the 6.5% SDS-PAGE. KaiA (0.9 μM), KaiB (3.4 μM), and KaiC (3.4 μM) are mixed to generate circadian oscillation and treated with oxidized quinone (9.6 μM) to generate the phase change. Dithionite (200 μM) was used to reduce quinone.

Source: P. Kim, Porr, et al., 2020

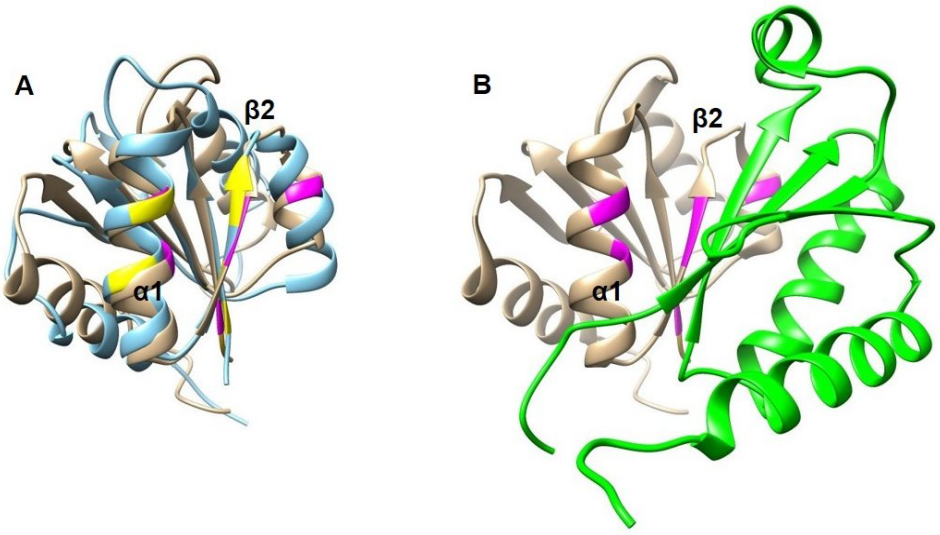

Figure A.6 Structures of CikA and KaiB.

(A) CikA from *Synechococcus elongatus* (PDBID: 2J48, cyan) is mapped with the disrupted residues (yellow) by quinone binding (Gao et al., 2007; Ivleva et al., 2006). CikA from *Thermosynechococcus elongatus* (PDBID: 5JYU, gold) is mapped with the residues (magenta) involved in binding to KaiB (Tseng et al., 2017). (B) The binding complex structure of CikA (gold) and KaiB (Green) (Tseng et al., 2017).
Source: P. Kim, Porr, et al., 2020

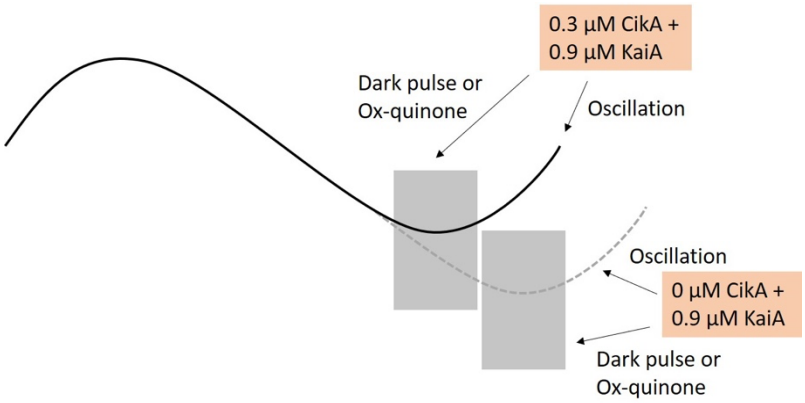

Figure A.7 Hypothetical mechanism of the phase delay in the circadian oscillation. When the dark pulse applied in the system with CikA (solid line), the system starts to follow the trajectory of the system without CikA (dotted line). This transition generates the phase delay.
Source: P. Kim, Porr, et al., 2020

APPENDIX B

SUPPLEMENTARY MATERIALS FOR CHAPTER 4

This appendix lists the figures that are supplementary to Chapter 4, Shift in Conformational Equilibrium Underlies the Oscillatory Phosphoryl Transfer Reaction of KaiC.

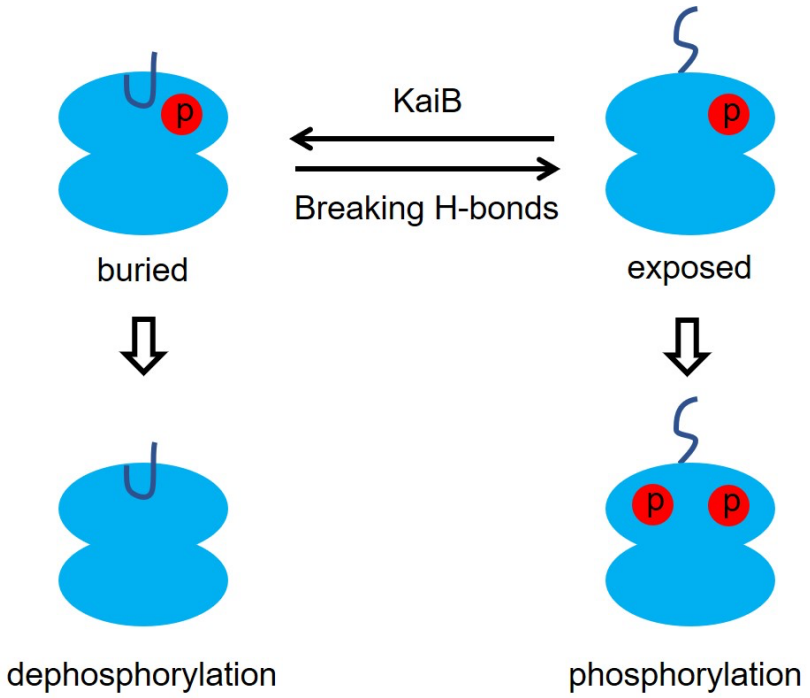

Figure B.1 The dynamic equilibrium of A-loop conformations. The A-loop conformations of KaiC change spontaneously in the regular reaction condition (Y. I. Kim et al., 2015). The buried conformation and exposed conformation induce the dephosphorylation and phosphorylation of KaiC, respectively (Y. I. Kim et al., 2008). The factors shifting the equilibrium were written on the arrows. P in the red circle represents two phosphorylation sites in KaiC monomer. One A-loop and two phosphorylation were drawn on the cartoon representation of KaiC hexamer for simplicity.
Source: P. Kim et al., Submitted

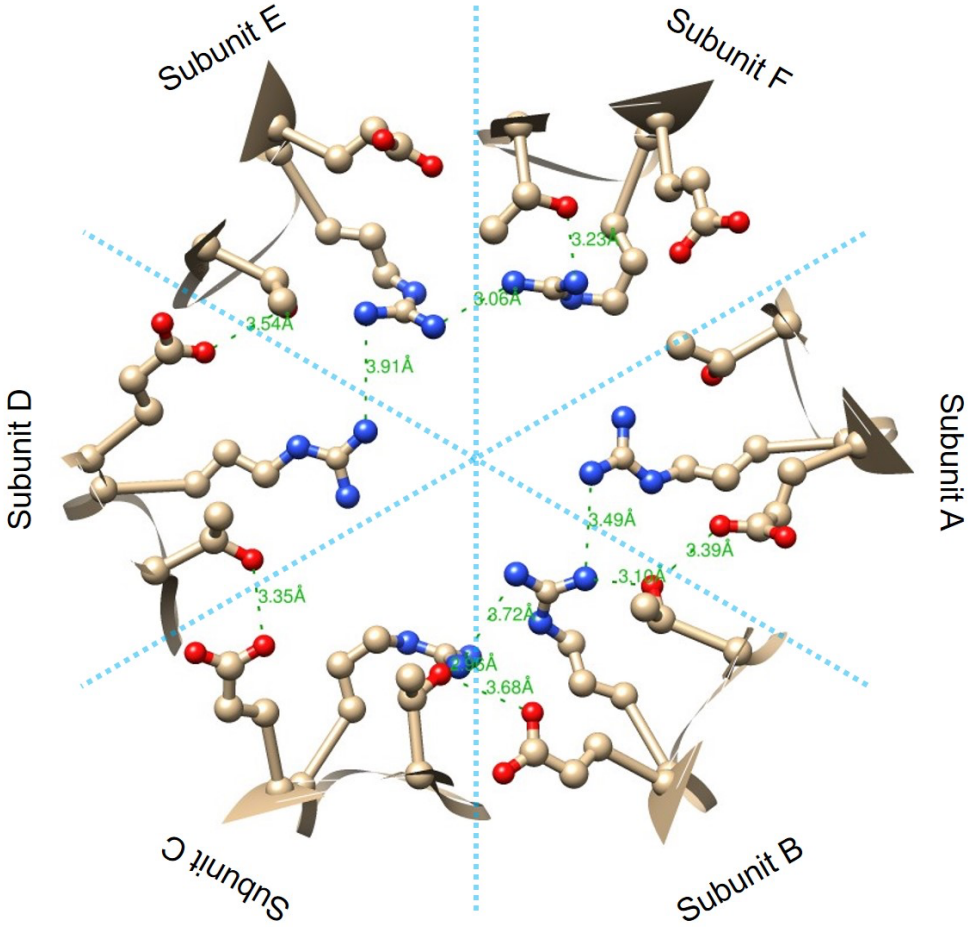

Figure B.2 The putative H-bond network of A-loops within the KaiC hexamer. The KaiC X-ray crystal structure (PDBID: 1TF7) was analyzed using UCSF Chimera (Pettersen et al., 2004). Each A-loop from monomer subunits is separated by blue dotted line for visibility. The atoms forming putative H-bonds are connected with green dotted lines. The distances are measured using the "Structure analysis – Distances" function in UCSF Chimera and labeled on the bonds.
Source: P. Kim et al., Submitted

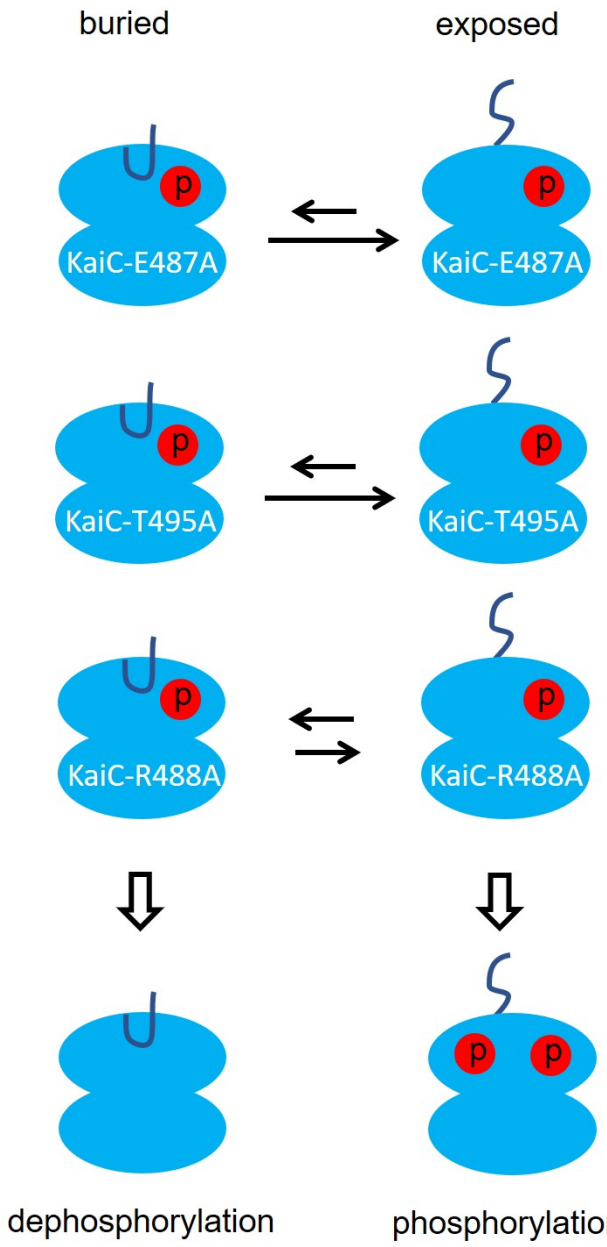

Figure B.3 The dynamic equilibrium of KaiC mutants. The hypothetical equilibrium shift corresponds to the length of the arrow. The equilibrium shifts were predicted with the phosphorylation state of each KaiC mutant.
Source: P. Kim et al., Submitted

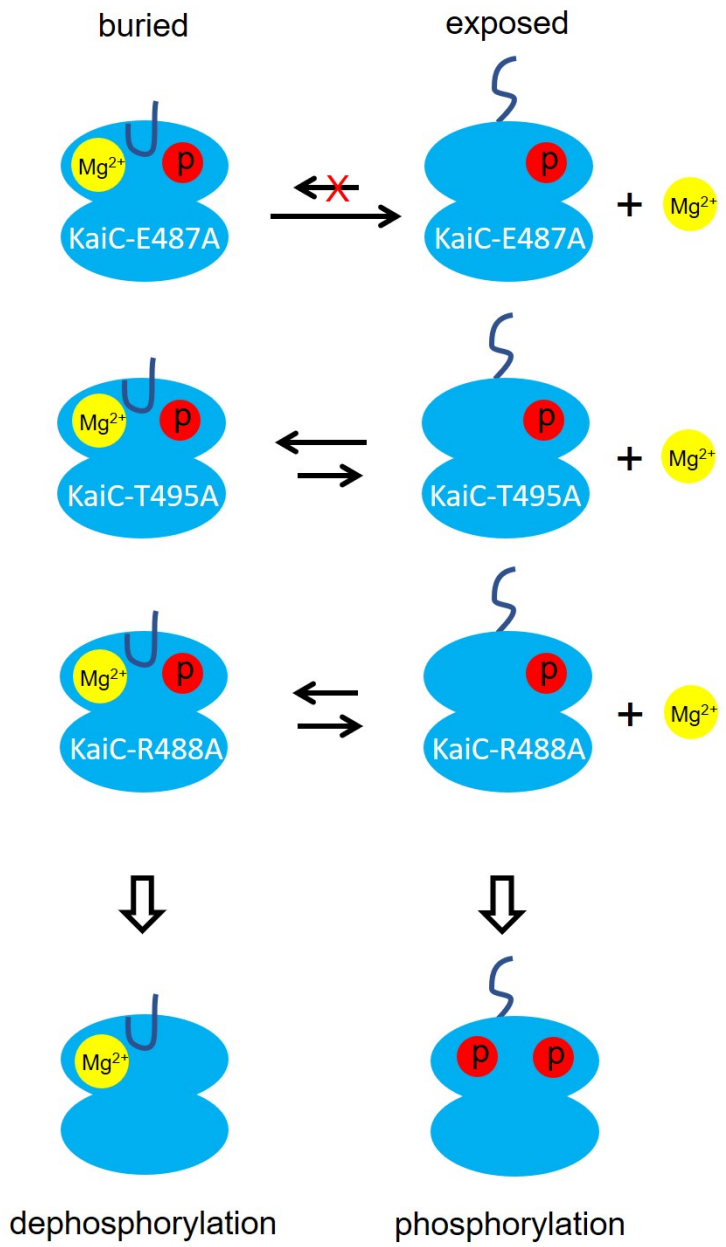

Figure B.4 The dynamic equilibrium of KaiC mutants in the presence of high Mg^{2+} concentration. The hypothetical equilibrium shift corresponds to the length of the arrow. The equilibrium shifts were predicted with the phosphorylation state of each KaiC mutant.

Source: P. Kim et al., Submitted

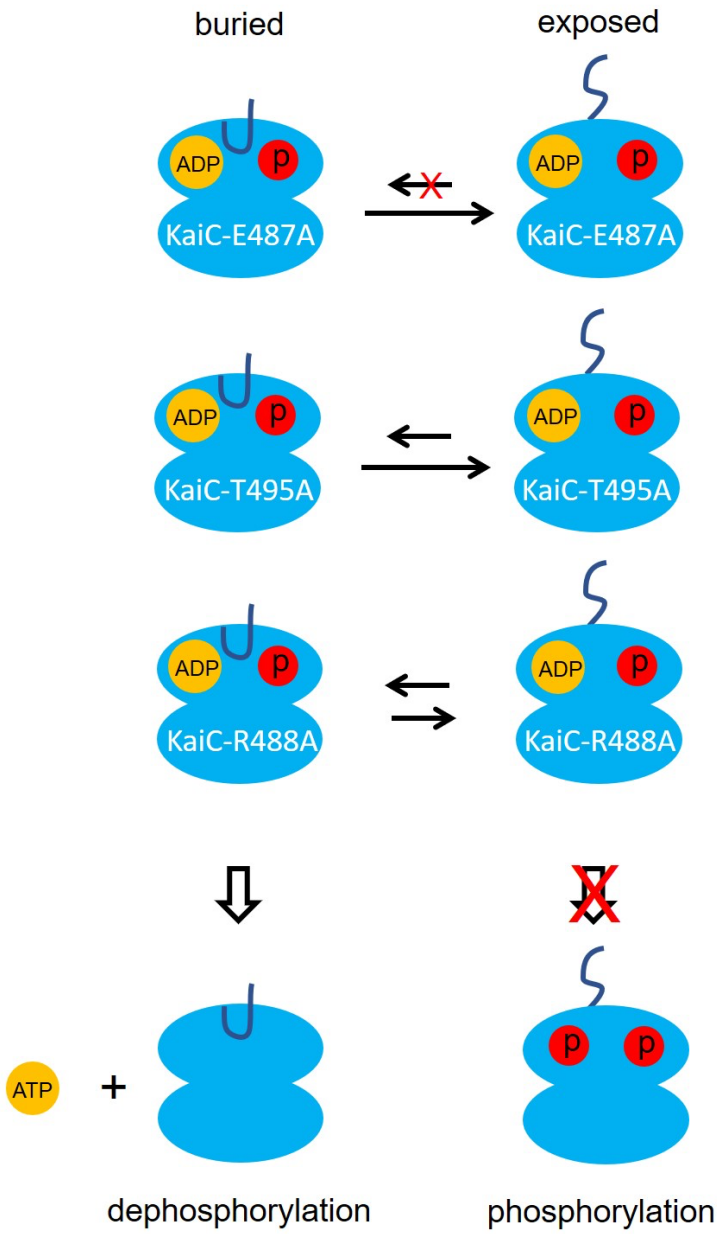

Figure B.5 The dynamic equilibrium of KaiC mutants in the presence of high ADP concentration. ADP binds both conformations. The phosphorylation is inhibited when ADP is bound in the exposed conformation. The dephosphorylation is induced by producing ATP when ADP is bound in the buried conformation.
Source: P. Kim et al., Submitted

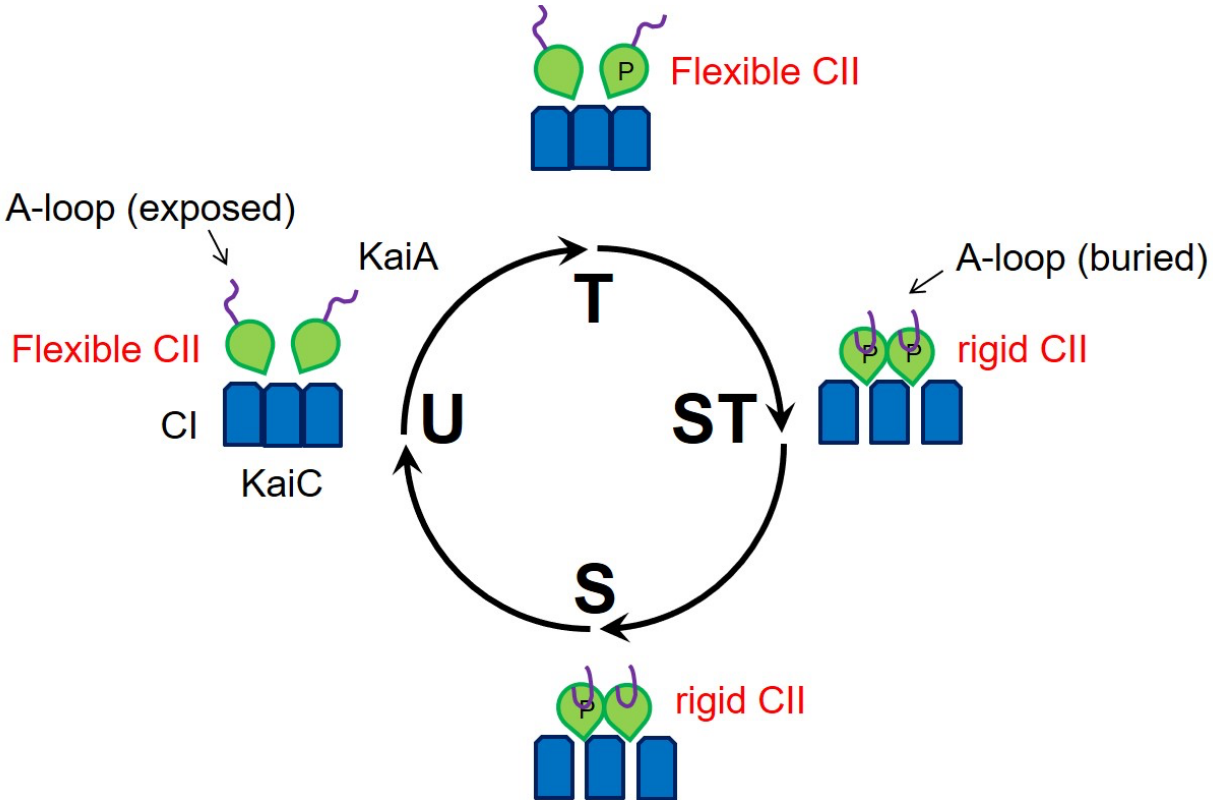

Figure B.6 The flexibility change of the CII domain of KaiC throughout each phosphorylation state. The CII domains of KaiC are flexible in the unphosphorylated KaiC (U). Throughout the phosphorylation phase, the CII domains remain flexible (U → T → ST). The flexible CII domains allow the A-loop to be exposed. When KaiC is fully phosphorylated, the A-loop switches to the buried conformation in the rigid CII domains (ST) until it becomes fully dephosphorylated (ST → S → U). The major phosphorylation states (black letters) of KaiC and the direction (black arrows) are denoted as a cycle. The KaiC conformations corresponding to the phosphorylation states are also shown. To simplify, only three subunits of CI domain and two subunits of CII domain were drawn.
Source: P. Kim et al., Submitted

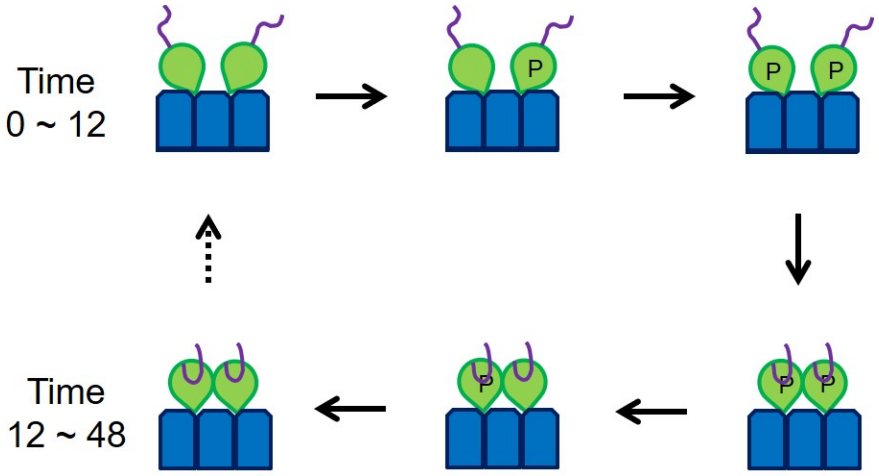

Figure B.7 A model of the conformational changes during the KaiC phosphorylation and dephosphorylation. The conformational changes in the CII domain and A-loop induce spontaneous phosphorylation and dephosphorylation. Green balloons represent the CII domain and their position shows their flexibility. The dotted arrow is a hypothetical pathway that is not observed in the experiment.
Source: P. Kim et al., Submitted

REFERENCES

Axmann, I. M., Hertel, S., Wiegard, A., Dorrich, A. K., & Wilde, A. (2014). Diversity of KaiC-based timing systems in marine Cyanobacteria. *Mar Genomics, 14*, 3-16. doi:10.1016/j.margen.2013.12.006

Chang, Y. G., Cohen, S. E., Phong, C., Myers, W. K., Kim, Y. I., Tseng, R., . . . LiWang, A. (2015). Circadian rhythms. A protein fold switch joins the circadian oscillator to clock output in cyanobacteria. *Science, 349*(6245), 324-328. doi:10.1126/science.1260031

Chang, Y. G., Kuo, N. W., Tseng, R., & LiWang, A. (2011). Flexibility of the C-terminal, or CII, ring of KaiC governs the rhythm of the circadian clock of cyanobacteria. *Proc Natl Acad Sci U S A, 108*(35), 14431-14436. doi:10.1073/pnas.1104221108

Chang, Y. G., Tseng, R., Kuo, N. W., & LiWang, A. (2012). Rhythmic ring-ring stacking drives the circadian oscillator clockwise. *Proc Natl Acad Sci U S A, 109*(42), 16847-16851. doi:10.1073/pnas.1211508109

Chen, Q., Liu, S., Yang, L., Zhang, L., & Li, J. (2018). The influence of KaiA mutations on its function in the KaiABC circadian clock system. *Data Brief, 18*, 241-247. doi:10.1016/j.dib.2018.03.032

Diamond, S., Rubin, B. E., Shultzaberger, R. K., Chen, Y., Barber, C. D., & Golden, S. S. (2017). Redox crisis underlies conditional light-dark lethality in cyanobacterial mutants that lack the circadian regulator, RpaA. *Proc Natl Acad Sci U S A, 114*(4), E580-E589. doi:10.1073/pnas.1613078114

Dong, G., Yang, Q., Wang, Q., Kim, Y. I., Wood, T. L., Osteryoung, K. W., . . . Golden, S. S. (2010). Elevated ATPase activity of KaiC applies a circadian checkpoint on cell division in Synechococcus elongatus. *Cell, 140*(4), 529-539. doi:10.1016/j.cell.2009.12.042

Ducat, D. C., Way, J. C., & Silver, P. A. (2011). Engineering cyanobacteria to generate high-value products. *Trends Biotechnol, 29*(2), 95-103. doi:10.1016/j.tibtech.2010.12.003

Dvornyk, V. (2009). The Circadian Clock Gear in Cyanobacteria: Assembled by Evolution. In J. L. Ditty, S. R. Mackey, & C. H. Johnson (Eds.), *Bacterial Circadian Programs* (pp. 241-258). Berlin, Heidelberg: Springer Berlin Heidelberg.

Dvornyk, V., Vinogradova, O., & Nevo, E. (2003). Origin and evolution of circadian clock genes in prokaryotes. *Proc Natl Acad Sci U S A, 100*(5), 2495-2500. doi:10.1073/pnas.0130099100

Egli, M., Mori, T., Pattanayek, R., Xu, Y., Qin, X., & Johnson, C. H. (2012). Dephosphorylation of the core clock protein KaiC in the cyanobacterial KaiABC circadian oscillator proceeds via an ATP synthase mechanism. *Biochemistry, 51*(8), 1547-1558. doi:10.1021/bi201525n

Egli, M., Pattanayek, R., Sheehan, J. H., Xu, Y., Mori, T., Smith, J. A., & Johnson, C. H. (2013). Loop-loop interactions regulate KaiA-stimulated KaiC phosphorylation in the cyanobacterial KaiABC circadian clock. *Biochemistry, 52*(7), 1208-1220. doi:10.1021/bi301691a

Escoubas, J. M., Lomas, M., LaRoche, J., & Falkowski, P. G. (1995). Light intensity regulation of cab gene transcription is signaled by the redox state of the plastoquinone pool. *Proc Natl Acad Sci U S A, 92*(22), 10237-10241. doi:10.1073/pnas.92.22.10237

Feeney, K. A., Hansen, L. L., Putker, M., Olivares-Yanez, C., Day, J., Eades, L. J., . . . van Ooijen, G. (2016). Daily magnesium fluxes regulate cellular timekeeping and energy balance. *Nature, 532*(7599), 375-379. doi:10.1038/nature17407

Förstner, U., & Wittmann, G. T. W. (1979). Metal Transfer Between Solid and Aqueous Phases. In U. Förstner & G. T. W. Wittmann (Eds.), *Metal Pollution in the Aquatic Environment* (pp. 197-270). Berlin, Heidelberg: Springer Berlin Heidelberg.

Gao, T., Zhang, X., Ivleva, N. B., Golden, S. S., & LiWang, A. (2007). NMR structure of the pseudo-receiver domain of CikA. *Protein Sci, 16*(3), 465-475. doi:10.1110/ps.062532007

Gutu, A., & O'Shea, E. K. (2013). Two antagonistic clock-regulated histidine kinases time the activation of circadian gene expression. *Mol Cell, 50*(2), 288-294. doi:10.1016/j.molcel.2013.02.022

Hong, L., Lavrentovich, D. O., Chavan, A., Leypunskiy, E., Li, E., Matthews, C., . . . Dinner, A. R. (2020). Bayesian modeling reveals metabolite-dependent ultrasensitivity in the cyanobacterial circadian clock. *Molecular Systems Biology, 16*(6), e9355. doi:10.15252/msb.20199355

Horita, J., Zimmermann, H., & Holland, H. D. (2002). Chemical evolution of seawater during the Phanerozoic: Implications from the record of marine evaporites. *Geochimica et Cosmochimica Acta, 66*(21), 3733-3756. doi:10.1016/S0016-7037(01)00884-5

Ishiura, M., Kutsuna, S., Aoki, S., Iwasaki, H., Andersson, C. R., Tanabe, A., . . . Kondo, T. (1998). Expression of a gene cluster kaiABC as a circadian feedback process in cyanobacteria. *Science, 281*(5382), 1519-1523.

Ito, H., Kageyama, H., Mutsuda, M., Nakajima, M., Oyama, T., & Kondo, T. (2007). Autonomous synchronization of the circadian KaiC phosphorylation rhythm. *Nat Struct Mol Biol, 14*(11), 1084-1088. doi:10.1038/nsmb1312

Ito, H., Mutsuda, M., Murayama, Y., Tomita, J., Hosokawa, N., Terauchi, K., . . . Iwasaki, H. (2009). Cyanobacterial daily life with Kai-based circadian and diurnal genome-wide transcriptional control in Synechococcus elongatus. *Proc Natl Acad Sci U S A, 106*(33), 14168-14173. doi:10.1073/pnas.0902587106

Ivleva, N. B., Bramlett, M. R., Lindahl, P. A., & Golden, S. S. (2005). LdpA: a component of the circadian clock senses redox state of the cell. *EMBO J, 24*(6), 1202-1210. doi:10.1038/sj.emboj.7600606

Ivleva, N. B., Gao, T., LiWang, A. C., & Golden, S. S. (2006). Quinone sensing by the circadian input kinase of the cyanobacterial circadian clock. *Proc Natl Acad Sci U S A, 103*(46), 17468-17473. doi:10.1073/pnas.0606639103

Iwasaki, H., Nishiwaki, T., Kitayama, Y., Nakajima, M., & Kondo, T. (2002). KaiA-stimulated KaiC phosphorylation in circadian timing loops in cyanobacteria. *Proc Natl Acad Sci U S A, 99*(24), 15788-15793. doi:10.1073/pnas.222467299

Jeong, Y. M., Dias, C., Diekman, C., Brochon, H., Kim, P., Kaur, M., . . . Kim, Y. I. (2019). Magnesium Regulates the Circadian Oscillator in Cyanobacteria. *J Biol Rhythms, 34*(4), 380-390. doi:10.1177/0748730419851655

Johnson, C. H. (1999). Forty years of PRCs--what have we learned? *Chronobiol Int, 16*(6), 711-743. doi:10.3109/07420529909016940

Johnson, C. H., Zhao, C., Xu, Y., & Mori, T. (2017). Timing the day: what makes bacterial clocks tick? *Nat Rev Microbiol, 15*(4), 232-242. doi:10.1038/nrmicro.2016.196

Kageyama, H., Nishiwaki, T., Nakajima, M., Iwasaki, H., Oyama, T., & Kondo, T. (2006). Cyanobacterial circadian pacemaker: Kai protein complex dynamics in the KaiC phosphorylation cycle in vitro. *Mol Cell, 23*(2), 161-171. doi:10.1016/j.molcel.2006.05.039

Kasting, J. F., & Siefert, J. L. (2002). Life and the evolution of Earth's atmosphere. *Science, 296*(5570), 1066-1068. doi:10.1126/science.1071184

Kaur, M., Ng, A., Kim, P., Diekman, C., & Kim, Y.-I. (2019). CikA Modulates the Effect of KaiA on the Period of the Circadian Oscillation in KaiC Phosphorylation. *J Biol Rhythms, 34*(2), 218-223. doi:10.1177/0748730419828068

Kaur, M., Ng, A., Kim, P., Diekman, C., & Kim, Y. I. (2019). CikA Modulates the Effect of KaiA on the Period of the Circadian Oscillation in KaiC Phosphorylation. *J Biol Rhythms, 34*(2), 218-223. doi:10.1177/0748730419828068

Kim, P., Kaszuba, A., Jang, H.-I., & Kim, Y.-I. (2020). Purification of GST-Fused Cyanobacterial Central Oscillator Protein KaiC. *Applied Biochemistry and Microbiology, 56*(4), 395–399.

Kim, P., Porr, B., Mori, T., Kim, Y. S., Johnson, C. H., Diekman, C. O., & Kim, Y. I. (2020). CikA, an Input Pathway Component, Senses the Oxidized Quinone Signal to Generate Phase Delays in the Cyanobacterial Circadian Clock. *J Biol Rhythms*, 748730419900868. doi:10.1177/0748730419900868

Kim, Y. I., Boyd, J. S., Espinosa, J., & Golden, S. S. (2015). Detecting KaiC phosphorylation rhythms of the cyanobacterial circadian oscillator in vitro and in vivo. *Methods Enzymol, 551*, 153-173. doi:10.1016/bs.mie.2014.10.003

Kim, Y. I., Dong, G., Carruthers, C. W., Jr., Golden, S. S., & LiWang, A. (2008). The day/night switch in KaiC, a central oscillator component of the circadian clock of cyanobacteria. *Proc Natl Acad Sci U S A, 105*(35), 12825-12830. doi:10.1073/pnas.0800526105

Kim, Y. I., Vinyard, D. J., Ananyev, G. M., Dismukes, G. C., & Golden, S. S. (2012). Oxidized quinones signal onset of darkness directly to the cyanobacterial circadian oscillator. *Proc Natl Acad Sci U S A, 109*(44), 17765-17769. doi:10.1073/pnas.1216401109

Kitayama, Y., Iwasaki, H., Nishiwaki, T., & Kondo, T. (2003). KaiB functions as an attenuator of KaiC phosphorylation in the cyanobacterial circadian clock system. *EMBO J, 22*(9), 2127-2134. doi:10.1093/emboj/cdg212

Kitayama, Y., Nishiwaki, T., Terauchi, K., & Kondo, T. (2008). Dual KaiC-based oscillations constitute the circadian system of cyanobacteria. *Genes Dev, 22*(11), 1513-1521. doi:10.1101/gad.1661808

Kiyohara, Y. B., Katayama, M., & Kondo, T. (2005). A novel mutation in kaiC affects resetting of the cyanobacterial circadian clock. *J Bacteriol, 187*(8), 2559-2564. doi:10.1128/JB.187.8.2559-2564.2005

Kondo, T., Strayer, C. A., Kulkarni, R. D., Taylor, W., Ishiura, M., Golden, S. S., & Johnson, C. H. (1993). Circadian rhythms in prokaryotes: luciferase as a reporter of circadian gene expression in cyanobacteria. *Proc Natl Acad Sci U S A, 90*(12), 5672-5676. Retrieved from https://www.ncbi.nlm.nih.gov/pubmed/8516317

Lea-Smith, D. J., Bombelli, P., Vasudevan, R., & Howe, C. J. (2016). Photosynthetic, respiratory and extracellular electron transport pathways in cyanobacteria. *Biochim Biophys Acta, 1857*(3), 247-255. doi:10.1016/j.bbabio.2015.10.007

Lyu, H., & Lazar, D. (2017). Modeling the light-induced electric potential difference DeltaPsi across the thylakoid membrane based on the transition state rate theory. *Biochim Biophys Acta Bioenerg, 1858*(3), 239-248. doi:10.1016/j.bbabio.2016.12.009

Ma, P., Mori, T., Zhao, C., Thiel, T., & Johnson, C. H. (2016). Evolution of KaiC-Dependent Timekeepers: A Proto-circadian Timing Mechanism Confers Adaptive Fitness in the Purple Bacterium Rhodopseudomonas palustris. *PLoS Genet, 12*(3), e1005922. doi:10.1371/journal.pgen.1005922

Mackey, S. R., Choi, J.-S., Kitayama, Y., Iwasaki, H., Dong, G., & Golden, S. S. (2008). Proteins Found in a CikA Interaction Assay Link the Circadian Clock, Metabolism, and Cell Division in <em>Synechococcus elongatus</em&gt. *Journal of Bacteriology, 190*(10), 3738. doi:10.1128/JB.01721-07

Markson, J. S., Piechura, J. R., Puszynska, A. M., & O'Shea, E. K. (2013). Circadian control of global gene expression by the cyanobacterial master regulator RpaA. *Cell, 155*(6), 1396-1408. doi:10.1016/j.cell.2013.11.005

Mittal, M. K., Misra, S., Owais, M., & Goyal, N. (2005). Expression, purification, and characterization of Leishmania donovani trypanothione reductase in Escherichia coli. *Protein Expr Purif, 40*(2), 279-286. doi:10.1016/j.pep.2004.12.012

Montgomery, B. L., & Lagarias, J. C. (2002). Phytochrome ancestry: sensors of bilins and light. *Trends Plant Sci, 7*(8), 357-366. doi:10.1016/s1360-1385(02)02304-x

Mori, T., Sugiyama, S., Byrne, M., Johnson, C. H., Uchihashi, T., & Ando, T. (2018). Revealing circadian mechanisms of integration and resilience by visualizing clock proteins working in real time. *Nat Commun, 9*(1), 3245. doi:10.1038/s41467-018-05438-4

Mukaiyama, A., Ouyang, D., Furuike, Y., & Akiyama, S. (2019). KaiC from a cyanobacterium Gloeocapsa sp. PCC 7428 retains functional and structural properties required as the core of circadian clock system. *Int J Biol Macromol, 131*, 67-73. doi:10.1016/j.ijbiomac.2019.03.051

Mullineaux, C. W. (2014). Co-existence of photosynthetic and respiratory activities in cyanobacterial thylakoid membranes. *Biochim Biophys Acta, 1837*(4), 503-511. doi:10.1016/j.bbabio.2013.11.017

Mutsuda, M., Michel, K. P., Zhang, X., Montgomery, B. L., & Golden, S. S. (2003). Biochemical properties of CikA, an unusual phytochrome-like histidine protein kinase that resets the circadian clock in Synechococcus elongatus PCC 7942. *J Biol Chem, 278*(21), 19102-19110. doi:10.1074/jbc.M213255200

Nakajima, M., Imai, K., Ito, H., Nishiwaki, T., Murayama, Y., Iwasaki, H., . . . Kondo, T. (2005). Reconstitution of circadian oscillation of cyanobacterial KaiC phosphorylation in vitro. *Science, 308*(5720), 414-415. doi:10.1126/science.1108451

Nakajima, M., Ito, H., & Kondo, T. (2010). In vitro regulation of circadian phosphorylation rhythm of cyanobacterial clock protein KaiC by KaiA and KaiB. *FEBS Lett, 584*(5), 898-902. doi:10.1016/j.febslet.2010.01.016

Nishiwaki, T., Iwasaki, H., Ishiura, M., & Kondo, T. (2000). Nucleotide binding and autophosphorylation of the clock protein KaiC as a circadian timing process of cyanobacteria. *Proc Natl Acad Sci U S A, 97*(1), 495-499. doi:10.1073/pnas.97.1.495

Nishiwaki, T., & Kondo, T. (2012). Circadian autodephosphorylation of cyanobacterial clock protein KaiC occurs via formation of ATP as intermediate. *J Biol Chem, 287*(22), 18030-18035. doi:10.1074/jbc.M112.350660

Nishiwaki, T., Satomi, Y., Kitayama, Y., Terauchi, K., Kiyohara, R., Takao, T., & Kondo, T. (2007). A sequential program of dual phosphorylation of KaiC as a basis for circadian rhythm in cyanobacteria. *EMBO J, 26*(17), 4029-4037. doi:10.1038/sj.emboj.7601832

Nishiwaki, T., Satomi, Y., Nakajima, M., Lee, C., Kiyohara, R., Kageyama, H., . . . Kondo, T. (2004). Role of KaiC phosphorylation in the circadian clock system of Synechococcus elongatus PCC 7942. *Proc Natl Acad Sci U S A, 101*(38), 13927-13932. doi:10.1073/pnas.0403906101

Nozzi, N., Oliver, J., & Atsumi, S. (2013). Cyanobacteria as a Platform for Biofuel Production. *Frontiers in Bioengineering and Biotechnology, 1*(7). doi:10.3389/fbioe.2013.00007

Ouyang, Y., Andersson, C. R., Kondo, T., Golden, S. S., & Johnson, C. H. (1998). Resonating circadian clocks enhance fitness in cyanobacteria. *Proc Natl Acad Sci U S A, 95*(15), 8660-8664. doi:10.1073/pnas.95.15.8660

Pattanayek, R., Mori, T., Xu, Y., Pattanayek, S., Johnson, C. H., & Egli, M. (2009). Structures of KaiC circadian clock mutant proteins: a new phosphorylation site at T426 and mechanisms of kinase, ATPase and phosphatase. *PLoS One, 4*(11), e7529. doi:10.1371/journal.pone.0007529

Pattanayek, R., Sidiqi, S. K., & Egli, M. (2012). Crystal structure of the redox-active cofactor dibromothymoquinone bound to circadian clock protein KaiA and structural basis for dibromothymoquinone's ability to prevent stimulation of KaiC phosphorylation by KaiA. *Biochemistry, 51*(41), 8050-8052. doi:10.1021/bi301222t

Pattanayek, R., Wang, J., Mori, T., Xu, Y., Johnson, C. H., & Egli, M. (2004). Visualizing a circadian clock protein: crystal structure of KaiC and functional insights. *Mol Cell, 15*(3), 375-388. doi:10.1016/j.molcel.2004.07.013

Pattanayek, R., Williams, D. R., Pattanayek, S., Xu, Y., Mori, T., Johnson, C. H., . . . Egli, M. (2006). Analysis of KaiA-KaiC protein interactions in the cyano-bacterial circadian clock using hybrid structural methods. *EMBO J, 25*(9), 2017-2028. doi:10.1038/sj.emboj.7601086

Pettersen, E. F., Goddard, T. D., Huang, C. C., Couch, G. S., Greenblatt, D. M., Meng, E. C., & Ferrin, T. E. (2004). UCSF Chimera--a visualization system for exploratory research and analysis. *J Comput Chem, 25*(13), 1605-1612. doi:10.1002/jcc.20084

Piechura, J. R., Amarnath, K., & O'Shea, E. K. (2017). Natural changes in light interact with circadian regulation at promoters to control gene expression in cyanobacteria. *Elife, 6*. doi:10.7554/eLife.32032

Pohland, A. C., & Schneider, D. (2019). Mg2+ homeostasis and transport in cyanobacteria - at the crossroads of bacterial and chloroplast Mg2+ import. *Biol Chem, 400*(10), 1289-1301. doi:10.1515/hsz-2018-0476

Puszynska, A. M., & O'Shea, E. K. (2017). Switching of metabolic programs in response to light availability is an essential function of the cyanobacterial circadian output pathway. *Elife, 6*. doi:10.7554/eLife.23210

Qin, X., Byrne, M., Mori, T., Zou, P., Williams, D. R., McHaourab, H., & Johnson, C. H. (2010). Intermolecular associations determine the dynamics of the circadian KaiABC oscillator. *Proc Natl Acad Sci U S A, 107*(33), 14805-14810. doi:10.1073/pnas.1002119107

Qin, X., Byrne, M., Xu, Y., Mori, T., & Johnson, C. H. (2010). Coupling of a core post-translational pacemaker to a slave transcription/translation feedback loop in a circadian system. *PLoS Biol, 8*(6), e1000394. doi:10.1371/journal.pbio.1000394

R Core Team. (2018). R: A language and environment for statistical computing. R Foundation for Statistical Computing, Vienna, Austria. https://www.R-project.org/.

Rial, D. V., & Ceccarelli, E. A. (2002). Removal of DnaK contamination during fusion protein purifications. *Protein Expression and Purification, 25*(3), 503-507. doi:https://doi.org/10.1016/S1046-5928(02)00024-4

Rust, M. J., Golden, S. S., & O'Shea, E. K. (2011). Light-driven changes in energy metabolism directly entrain the cyanobacterial circadian oscillator. *Science, 331*(6014), 220-223. doi:10.1126/science.1197243

Rust, M. J., Markson, J. S., Lane, W. S., Fisher, D. S., & O'Shea, E. K. (2007). Ordered phosphorylation governs oscillation of a three-protein circadian clock. *Science, 318*(5851), 809-812. doi:10.1126/science.1148596

Schindelin, J., Arganda-Carreras, I., Frise, E., Kaynig, V., Longair, M., Pietzsch, T., . . . Cardona, A. (2012). Fiji: an open-source platform for biological-image analysis. *Nat Methods, 9*(7), 676-682. doi:10.1038/nmeth.2019

Schmitz, O., Katayama, M., Williams, S. B., Kondo, T., & Golden, S. S. (2000). CikA, a bacteriophytochrome that resets the cyanobacterial circadian clock. *Science, 289*(5480), 765-768. doi:10.1126/science.289.5480.765

Shah, V., Garg, N., & Madamwar, D. (2001). An integrated process of textile dye removal and hydrogen evolution using cyanobacterium, Phormidium valderianum. *World Journal of Microbiology and Biotechnology, 17*(5), 499-504. doi:10.1023/A:1011994215307

Signorell, A., Aho, K., Anderegg, N., Aragon, T., Arppe, A., & Baddeley, A. (2019). DescTools: Tools for descriptive statistics. R package version 0.99.30.

Snijder, J., Burnley, R. J., Wiegard, A., Melquiond, A. S. J., Bonvin, A. M. J. J., Axmann, I. M., & Heck, A. J. R. (2014). Insight into cyanobacterial circadian timing from structural details of the KaiB–KaiC interaction. *Proc Natl Acad Sci U S A, 111*(4), 1379. doi:10.1073/pnas.1314326111

Takai, N., Nakajima, M., Oyama, T., Kito, R., Sugita, C., Sugita, M., . . . Iwasaki, H. (2006). A KaiC-associating SasA-RpaA two-component regulatory system as a major circadian timing mediator in cyanobacteria. *Proc Natl Acad Sci U S A, 103*(32), 12109-12114. doi:10.1073/pnas.0602955103

Taniguchi, Y., Takai, N., Katayama, M., Kondo, T., & Oyama, T. (2010). Three major output pathways from the KaiABC-based oscillator cooperate to generate robust circadian kaiBC expression in cyanobacteria. *Proc Natl Acad Sci U S A, 107*(7), 3263-3268. doi:10.1073/pnas.0909924107

Teng, S. W., Mukherji, S., Moffitt, J. R., de Buyl, S., & O'Shea, E. K. (2013). Robust circadian oscillations in growing cyanobacteria require transcriptional feedback. *Science, 340*(6133), 737-740. doi:10.1126/science.1230996

Tomita, J., Nakajima, M., Kondo, T., & Iwasaki, H. (2005). No transcription-translation feedback in circadian rhythm of KaiC phosphorylation. *Science, 307*(5707), 251-254. doi:10.1126/science.1102540

Tseng, R., Chang, Y. G., Bravo, I., Latham, R., Chaudhary, A., Kuo, N. W., & Liwang, A. (2014). Cooperative KaiA-KaiB-KaiC interactions affect KaiB/SasA competition in the circadian clock of cyanobacteria. *J Mol Biol, 426*(2), 389-402. doi:10.1016/j.jmb.2013.09.040

Tseng, R., Goularte, N. F., Chavan, A., Luu, J., Cohen, S. E., Chang, Y. G., . . . Partch, C. L. (2017). Structural basis of the day-night transition in a bacterial circadian clock. *Science, 355*(6330), 1174-1180. doi:10.1126/science.aag2516

Utkilen, H. C. (1982). Magnesium-limited Growth of the Cyanobacterium Anacystis nidulans. *Microbiology, 128*(8), 1849-1862. doi:10.1099/00221287-128-8-1849

Vakonakis, I., & LiWang, A. C. (2004). Structure of the C-terminal domain of the clock protein KaiA in complex with a KaiC-derived peptide: implications for KaiC regulation. *Proc Natl Acad Sci U S A, 101*(30), 10925-10930. doi:10.1073/pnas.0403037101

Vakonakis, I., Sun, J., Wu, T., Holzenburg, A., Golden, S. S., & LiWang, A. C. (2004). NMR structure of the KaiC-interacting C-terminal domain of KaiA, a circadian clock protein: implications for KaiA-KaiC interaction. *Proc Natl Acad Sci U S A, 101*(6), 1479-1484. doi:10.1073/pnas.0305516101

Vijayan, V., Zuzow, R., & O'Shea, E. K. (2009). Oscillations in supercoiling drive circadian gene expression in cyanobacteria. *Proc Natl Acad Sci U S A, 106*(52), 22564-22568. doi:10.1073/pnas.0912673106

Waldron, K. J., Rutherford, J. C., Ford, D., & Robinson, N. J. (2009). Metalloproteins and metal sensing. *Nature, 460*(7257), 823-830. doi:10.1038/nature08300

Williams, S. B., Vakonakis, I., Golden, S. S., & LiWang, A. C. (2002). Structure and function from the circadian clock protein KaiA of Synechococcus elongatus: a potential clock input mechanism. *Proc Natl Acad Sci U S A, 99*(24), 15357-15362. doi:10.1073/pnas.232517099

Wood, T. L., Bridwell-Rabb, J., Kim, Y.-I., Gao, T., Chang, Y.-G., LiWang, A., . . . Golden, S. S. (2010). The KaiA protein of the cyanobacterial circadian oscillator is modulated by a redox-active cofactor. *Proc Natl Acad Sci U S A, 107*(13), 5804-5809. doi:10.1073/pnas.0910141107

Xu, Y., Mori, T., & Johnson, C. H. (2003). Cyanobacterial circadian clockwork: roles of KaiA, KaiB and the kaiBC promoter in regulating KaiC. *EMBO J, 22*(9), 2117-2126. doi:10.1093/emboj/cdg168

Zhang, X., Dong, G., & Golden, S. S. (2006). The pseudo-receiver domain of CikA regulates the cyanobacterial circadian input pathway. *Mol Microbiol, 60*(3), 658-668. doi:10.1111/j.1365-2958.2006.05138.x

Zielinski, T., Moore, A. M., Troup, E., Halliday, K. J., & Millar, A. J. (2014). Strengths and limitations of period estimation methods for circadian data. *PLoS One, 9*(5), e96462. doi:10.1371/journal.pone.0096462